

1 **Enviro-HIRLAM online integrated meteorology-chemistry modelling system: strategy, methodology, developments** 2 **and applications (v. 7.2)**

3
4 *Alexander Baklanov (1, a), Ulrik Smith Korsholm (1), Roman Nuterman (2), Alexander Mahura (1, b), Kristian Pagh Nielsen*
5 *(1), Bent Hansen Sass (1), Alix Rasmussen (1), Ashraf Zahey (1, c), Eigil Kaas (2), Alexander Kurganskiy (2,3), Brian*
6 *Sørensen (2), Iratxe González-Aparicio (4)*

7
8 (1) Danish Meteorological Institute (DMI), Copenhagen, Denmark; (2) Niels Bohr Institute, University of
9 Copenhagen, Denmark; (3) Russian State Hydrometeorological University, St.Petersburg, Russia; (4) European
10 Commission, DG - Joint Research Centre, Institute for Energy and Transport, The Netherlands; (a) now at: World
11 Meteorological Organization (WMO), Geneva, Switzerland; (b) now at: University of Helsinki, Finland; (c) now
12 at: The Egyptian Meteorological Authority, Cairo, Egypt.

13
14 *Corresponding author email: abaklanov@wmo.int; alb@dmu.dk*

15
16
17 **Abstract:** The Environment – High Resolution Limited Area Model (Enviro-HIRLAM) is developed as a fully online
18 integrated numerical weather prediction (NWP) and atmospheric chemical transport (ACT) model for research and
19 forecasting of joint meteorological, chemical and biological weather. The integrated modelling system is developed by DMI
20 in collaboration with several European universities. It is the baseline system in the HIRLAM Chemical Branch and used in
21 several countries and different applications. The development was initiated at DMI more than 15 years ago. The model is
22 based on the HIRLAM NWP model with online integrated pollutant transport and dispersion, chemistry, aerosol dynamics,
23 deposition and atmospheric composition feedbacks. To make the model suitable for chemical weather forecasting in urban
24 areas the meteorological part was improved by implementation of urban parameterizations. The dynamical core was
25 improved by implementing a locally mass conserving semi-Lagrangian numerical advection scheme, which improves
26 forecast accuracy and model performance. The current version 7.2, in comparison with previous versions, has a more
27 advanced and cost-efficient chemistry, aerosol multi-compound approach, aerosol feedbacks (direct and semi-direct) on
28 radiation and (first and second indirect effects) on cloud microphysics. Since 2004 the Enviro-HIRLAM is used for different
29 studies, including operational pollen forecasting for Denmark since 2009, and operational forecasting atmospheric
30 composition with downscaling for China since 2017. Following main research and development strategy the further model
31 developments will be extended towards the new NWP platform - HARMONIE. Different aspects of online coupling
32 methodology, research strategy and possible applications of the modelling system, and ‘fit-for-purpose’ model configurations
33 for the meteorological and air quality communities are discussed.

34 35 36 **1. Introduction**

37
38 During the last decades a new field of atmospheric modelling - the chemical weather forecasting (CWF) - is quickly
39 developing and growing. However, in most of the current studies this field is still considered in a simplified concept of the
40 off-line running of atmospheric chemical transport (ACT) models with operational numerical weather prediction (NWP) data
41 as a driver (Lawrence et al., 2005). A new concept and methodology considering the “chemical weather” as two-way
42 interacting nonlinear meteorological and chemical/aerosol dynamics processes of the atmosphere have been recently
43 suggested (Grell et al., 2005; Baklanov and Korsholm, 2008; Baklanov, 2010; Grell and Baklanov, 2011). First attempts at
44 building online coupled meteorology and air pollution models for environmental applications were done in the 1980s, cf.
45 Baklanov (1988), Schlünzen and Pahl (1992), Jacobson (1994). For climate applications the first coupled chemistry-climate
46 models were developed and used in the 1990s, cf. Jacobson (1999, 2002), de Grandpré et al. (2000), Steil et al. (2003),
47 Austin and Butchart (2003). More detailed overview of the history and current experience in the online integrated
48 meteorology-chemistry modelling, importance of different chains of feedback mechanisms for meteorological and
49 atmospheric composition processes are discussed for USA (Zhang, 2008) and European (Baklanov et al., 2014) models.
50 Klein et al. (2012) extended applications of coupled models for "biological weather", defined as “the short-term state and
51 variation of concentrations of bioaerosols”, in particular for pollen modelling and forecasting.

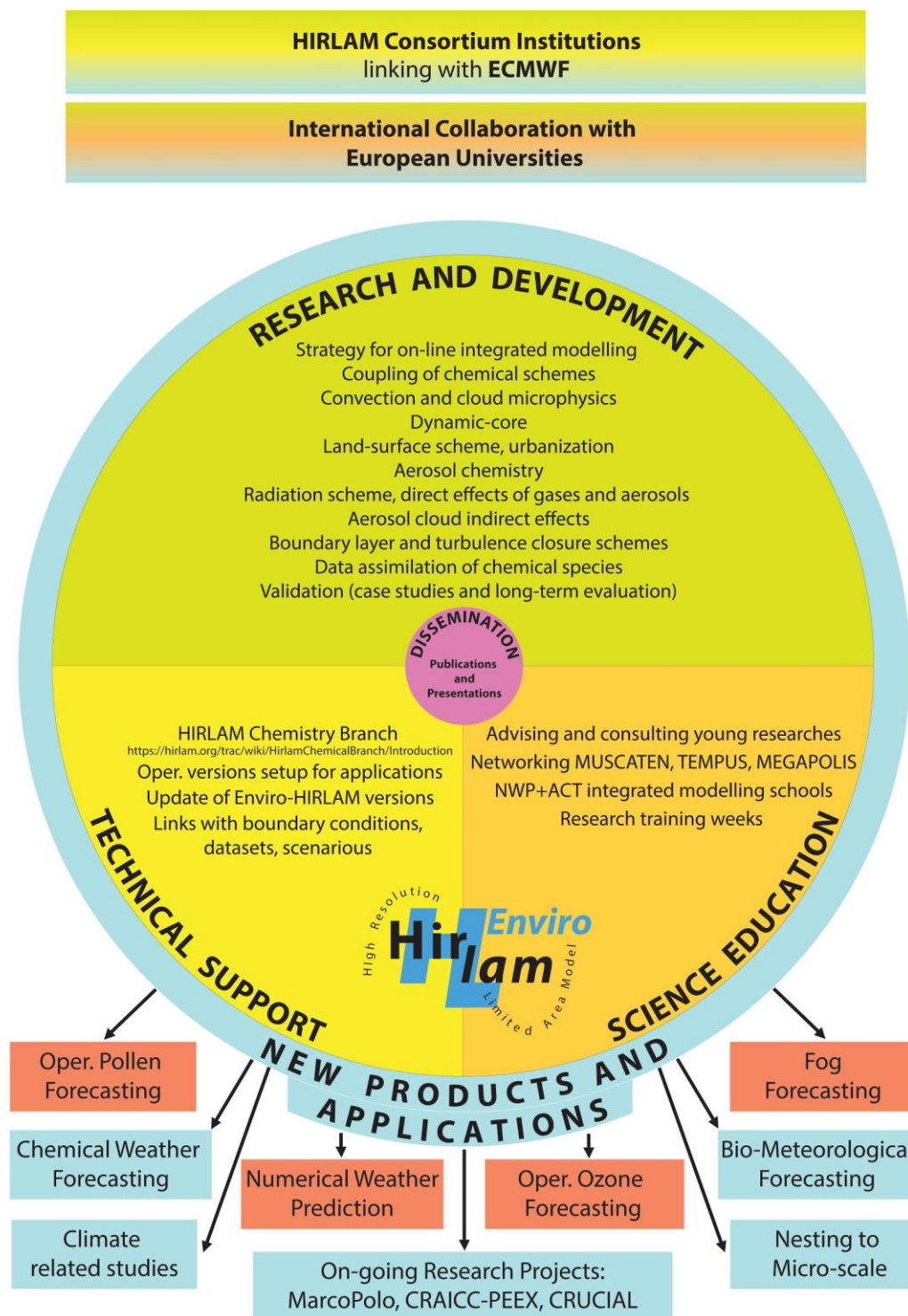
52 The online integration of meso-meteorological models (MetM) and atmospheric aerosols and ACT models gives a possibility
53 to utilize all meteorological 3D fields in the ACT model at each time step and to consider nonlinear feedbacks of air pollution
54 (e.g. atmospheric aerosols) on meteorological processes / climate forcing and then on the chemical composition of the
55 atmosphere. This very promising way for future atmospheric modelling systems (as a part of and a step toward the Earth
56 System Modelling, ESM) will lead to a new generation of seamless coupled models for meteorological, chemical and
57 biochemical weather forecasting. Seamless approach for ‘one atmosphere’ integrated meteorology-chemistry/aerosols
58 forecasting systems is analysed by the COST Action ES1004 EuMetChem (see e.g. Baklanov et al., 2015) and overview of
59 the current state of online coupled chemistry-meteorology models and needs for further developments were published in
60 (Zhang, 2008; WMO, 2016; Baklanov et al., 2017; Sokhi et al. 2017).

61 The methodology on how to realize the suggested integrated concept was demonstrated on an European example of the
62 Enviro-HIRLAM (Environment – High Resolution Limited Area Model) integrated modelling system (Baklanov et al.,
63 2008a; Korsholm, 2009). Experience from first HIRLAM community attempts to include pollutants into the NWP model
64 (Ekman, 2000) and from pioneering online coupled meteorology-pollution model developments of the Novosibirsk science

65
66
67
68
69
70
71
72

school (Marchuk, 1986; Penenko and Aloyan, 1985; Baklanov, 1988) was actively used for developments of the Enviro-HIRLAM modelling system.

The Enviro-HIRLAM is developed as a fully online integrated NWP and ACT modelling system for research and forecasting of meteorological, chemical and biological weather. The integrated modelling system is developed by DMI and other collaborators (Chenevez et al., 2004; Baklanov et al., 2008a, 2011b; Korsholm et al., 2008, 2009; Korsholm, 2009) and included as the baseline system of the Chemical Branch of the HIRLAM consortium (Figure 1).



73
74
75
76
77

Figure 1. General scheme of international collaboration, research and development, technical support and science education for the online integrated Enviro-HIRLAM: ‘Environment – HIgh Resolution Limited Area Model’.

78
79 The model development was initiated at DMI more than 15 years ago and it is used now in several countries. The modelling
80 system is being used for different completed and ongoing research projects (FP6 FUMAPEX; FP7 MEGAPOLI, PEGASOS,
81 MACC, TRANSPHORM, MarcoPolo; NordForsk NetFAM, MUSCATEN, CarboNord, CRAICC-PEEX, CRUCIAL; COST
82 Actions – 728, 732, ES0602 ENCWF, ES1004 EuMetChem), and for operational pollen forecasting in Denmark since 2009
83 (Rasmussen et al., 2006; Mahura et al., 2006b) and operational atmospheric composition (with focus on aerosols) for China
84 since Nov 2016 (Mahura et al., 2016; 2017). Following main strategic plans (Baklanov, 2008; Baklanov et al., 2011a) within
85 HIRLAM-B,-C projects further developments of the modelling system will be shifting to new NWP platform (from
86 HIRLAM to HARMONIE) and a close collaboration with the ALADIN (Aire Limitée Adaptation dynamique
87 Développement InterNational) community was initiated in 2014.
88

89 In this paper an overall description of the current version of the Enviro-HIRLAM coupled modelling system with improved
90 parameterisations of meteorology-composition two-way interactions, main steps in its development and examples in different
91 application areas for air quality, weather and pollen forecasting are considered for the first time. Section 2 provides a detailed
92 description of the Enviro-HIRLAM modelling system and its key developments in the meteorological core, chemistry and
93 aerosol dynamics parts, aerosol-meteorology interactions, models urbanisation and improvements of numerical algorithms.
94 Section 3 describes a few types of Enviro-HIRLAM applications for meteorological and environmental forecasting and
95 assessment studies. Sections 4 and 5 continue discussions and summarise the model applicability and provide
96 recommendations for future research. Annex 1 includes brief information about the Enviro-HIRLAM model development
97 history. A list of acronyms is provided in Annex 2.
98

99 **2. Enviro-HIRLAM modelling system description**

100 **2.1. Modelling system structure**

101
102 The Enviro-HIRLAM is a fully online coupled (integrated) NWP and ACT modelling system for research and forecasting of
103 meteorological, chemical and biological weather (see schematics in Figure 2). The modelling system was originally
104 developed by DMI and further with other collaborators, and now it is included by the European HIRLAM consortium as a
105 baseline system in the HIRLAM Chemical Branch (<http://hirlam.org/index.php/documentation/chemistry-branch>). It was the
106 first meso-scale online coupled model in Europe that considered two-way indirect feedbacks between meteorology and
107 chemistry/aerosols (WMO-COST, 2008).
108

109 The following main steps of the model development were realised such as: (i) model nesting for high resolutions, (ii)
110 improved resolving PBL and surface layer structure, (iii) urbanisation of the NWP model, (iv) improvement of advection
111 schemes, (v) emission inventories and models, (vi) implementation of gas-phase chemistry mechanisms, (vii) implementation
112 of aerosol dynamics, (viii) realisation of aerosol feedback mechanisms.
113

114 The first version was based on the DMI-HIRLAM NWP model with online integrated pollutant transport and dispersion
115 (Chenevez et al., 2004), chemistry, deposition and indirect effects (Korsholm et al., 2008; Korsholm, 2009) and later aerosol
116 (only for sulphur particles) dynamics (Baklanov, 2003; Gross and Baklanov, 2004). To make the model suitable for chemical
117 weather forecasting in urban areas the meteorological part was improved by implementation of urban sub-layer
118 parameterisations (Baklanov et al., 2008b; Mahura et al., 2008a; González-Aparicio et al., 2013). The model's dynamic core
119 was improved by adding a locally mass conserving semi-Lagrangian numerical advection scheme (Kaas, 2008; Sørensen,
120 2012; Sørensen et al., 2013), which improves forecast accuracy and enables performing longer runs. More details of the
121 system development history is presented in the Annex 1.

122 The current version of Enviro-HIRLAM (Nuterman et al., 2013; Nuterman et al., 2015) is based on the reference HIRLAM
123 v7.2 with a more advanced and effective chemistry scheme, multi-compound modal approach aerosol dynamics modules,
124 aerosol feedbacks on radiation (direct and semi-direct effects) and on cloud microphysics (first and second indirect effects).
125 This version is continuously under development and evaluation for various weather and air quality related applications (in
126 particular, within the COST Action ES1004 where the above mentioned effects were extensively discussed, see, e.g., in
127 Baklanov et al. 2014).
128

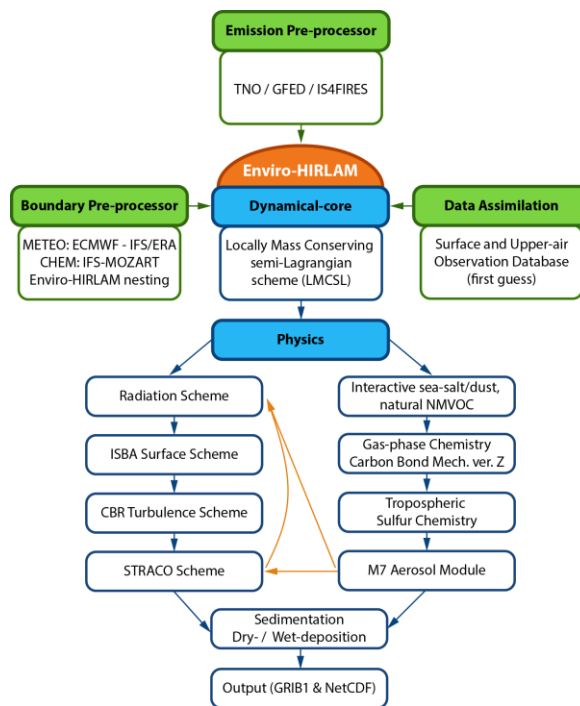


Figure 2: Schematics of the Enviro-HIRLAM modelling system.

Vertical and horizontal resolutions of the model are flexible. Limitations, e.g. due to the hydrostatic approximation, are provided (min 1,5 km of the horizontal resolution for flat terrains, e.g. for Copenhagen).

2.2. Meteorological core of the system

The first version of Enviro-HIRLAM was based on a previous version HIRLAM-tracer and at its meteorological core lies DMI-HIRLAM, version 6.3.7 employed for limited area short range operational weather forecasting at DMI (Chenevez et al., 2004). The current model version used in studies is based on the reference version of the HIRLAM community meteorological NWP model HIRLAM version 7.2 and online-coupled environmental block (so-called, the Enviro-) allowing to take into account spatial-temporal evolution of atmospheric chemical and biological aerosols driven by meteorology from NWP block.

HIRLAM is a hydrostatic NWP model which is used for both research and operational purposes. The model provides forecast of main meteorological fields, including: air temperature and specific humidity, atmospheric pressure, wind speed and direction, cloud cover and turbulent kinetic energy (TKE) based on forward in time integration of the primitive equations (dynamical core) (Holton, 2004) and physical processes such as radiation, vertical diffusion, convection, condensation, etc. (physical core).

The detailed NWP HIRLAM description can be found in the HIRLAM reference guide science documentation (Undén et al., 2002) and its following upgrades and modifications (see more details at <http://www.hirlam.org>).

The hydrostatic approximation of the model can be a limitation to increase the resolution for urban simulations. However, sensitivity tests for a medium size city demonstrated that the 2.5 km was the optimal resolution, allowing at the same time to obtain satisfactory reproducibility of the large scale processes and to explore the urban effects at local scale (González-Aparicio et al. 2013). For other metropolitan areas such as Paris, Rotterdam, St. Petersburg, Shanghai - a similar resolution was chosen, whereas for Copenhagen (with its flat terrain) the highest suitable resolution tested was 1.5 km and provided reasonable verification results (Mahura et al., 2006a, 2008bc, 2016). Within a selected metropolitan area there could be only a few grid cells having 100% representation of the urban fraction, but taking into account all urban grid cells, the boundaries of the cities (number of cells) could be substantially larger. Moreover, most of existing parameterizations in the physics core of any NWP model might need a revision when resolutions of 1 km and finer are used.

Following the main strategic development within HIRLAM (HIRLAM-B and -C projects), there are plans for further developments of Enviro-HIRLAM shifting to new non-hydrostatic NWP platform (e.g. HARMONIE model) and incorporating chemistry modules and aerosol-radiation-cloud interactions into the future integrated system (Baklanov, 2008; Baklanov et al., 2011a).

The new non-hydrostatic version under HARMONIE is under development and only some elements are realised so far. The non-hydrostatic HARMONIE-AROME model includes only some aerosol effects. The physics included in this version of HARMONIE has recently been detailed by Bengtsson et al. (2017). HARMONIE-AROME is based partly on Meso-NH (Mesoscale Non-Hydrostatic atmospheric model), which is a cloud resolving model that includes state-of-the-art chemistry and aerosol interactions (e.g. Berger et al. 2016). However, Meso-NH cannot be run as a near real time NWP model, as it is possible with Enviro-HIRLAM.

2.3. Atmospheric chemistry

a) Tropospheric Sulfur Cycle

The simple tropospheric sulphur cycle chemistry module in Enviro-HIRLAM, used for long-term runs (up to one year), is based on the sulfur cycle mechanism developed by Feichter et al. (1996) treating three prognostic species dimethyl sulfide (DMS), sulfur dioxide (SO₂) and sulfate (SO₄²⁻). The mechanism includes DMS and SO₂ oxidation by hydroxyl (OH) and DMS reactions with nitrate radicals (NO₃) in the gas-phase part. The heterogeneous aqueous phases chemistry comprises of SO₂ oxidation reactions by H₂O₂ and O₃. Accounting for dissolution effects of SO₂ in the aqueous phase is performed according to Henry's law. An output of global chemistry transport model MOZART (Horowitz et al., 2003) is used to prescribe three dimensional oxidant fields of OH, H₂O₂, NO₂, and O₃.

The sulfate produced in the gas-phase is referred to the gases and can be condensed on pre-existing aerosols or to nucleate by the aerosol microphysics M7 module (see Sect. 2.4). Moreover, in-cloud produced sulfate is accumulated on the pre-existing accumulation and coarse mode aerosols.

The tropospheric sulfur cycle chemistry is used together with M7 aerosol microphysics module because of its relative simplicity and low computational cost. The CBM-Z gas-phase chemistry (see the next section) is not interfaced with the M7 aerosol module because of several reasons: 1) the aerosol microphysics module does not include Secondary Organic Aerosols, therefore, there is no need of complex gas-phase mechanism with Volatile Organic Compounds related reactions and 2) it is too computationally expensive to use CBM-Z together with M7 for both weather and atmospheric composition prediction.

b) Gas-phase chemistry

The gas-phase chemistry scheme consists of sets of chemical schemes running from simple schemes for Chemical Weather Forecasts to highly complex schemes for research and case studies. In order to make the model computationally efficient for different applications and operational forecasting several condensed atmospheric chemical schemes have been tested into Enviro-HIRMAM since the first version of the model system was realised (Korsholm, 2009; Gross and Baklanov 2004). In the current version of Enviro-HIRLAM the tropospheric condensed Carbon-Bond Mechanism version Z (CBM-Z) (Zaveri and Peters, 1999), a variant of CBM-IV gas-phase chemistry scheme (Gery et al., 1989), with a fast solver based on radical balances (Sandu et al., 2006) has been implemented in the model. CBM-Z uses lumped species that represent broad categories of organics based on carbon bond structure. It is closely related to CBM-IV which is widely used in air pollution evaluations, but with expansions to include reactions that are important in the remote troposphere. It also uses the most general organic category (PAR for paraffin) to represent miscellaneous carbon content so that carbon mass is conserved.

Six environmental/smog chamber experiments were used to validate the gas-phase schemes as box models and within a regional climate model (Shalaby, 2012; Shalaby et al., 2012). The Tennessee Valley Authority (TVA) and the EPA chamber experiments were used to evaluate the different gas-phase schemes and different chemical solvers. Namely, TVA005 and TVA006 are designed to test the simple system of NO_x; TVA068 is designed to test a simple mixture of VOC with very high NO_x. EPA069A, EPA073A and EPA150A are used to validate the schemes with low NO_x concentration and high VOC concentration.

c) Chemical Solvers

Calculating the time evolution of gas-phase chemistry requires a numerical integration of a set of stiff ordinary differential equations (ODE) and is among the most computationally expensive operations performed in a photochemical grid model. The equations for photochemical production and loss are computationally expensive because they form a stiff numerical system. The photochemical mechanisms described above were implemented using two different chemical solvers to solve the tendency equation for photochemical production and loss: (1) the Rosenbrock (ROS) solver (Sandu et al., 1997 and Hairer and Wanner, 1996) as implemented by the Kinetic Preprocessor (KPP) (Sandu et al., 2006); and (2) the computationally rapid radical balance method (RBM) of (Sillman, 1991). RBM utilizes the fact that much of the complexity of tropospheric chemistry stems from the HO_x radical family (OH, HO₂ and RO₂), which has a limited set of sources and sinks. The method solves reverse-Euler equations for OH and HO₂ based on the balance between sources, sinks and (if applicable) prior concentrations at the start of the time step. Reverse Euler equations for other species are solved in a reactant-to-product order, in some cases involving pairs of rapidly interacting species, and with some modifications to increase accuracy in exponential decay situations. The procedure is equivalent to a reverse Euler solution using sparse-matrix techniques, but with the matrix inversion linked specifically to the behaviour of OH and other species in the troposphere. Prior work tested several atmospheric chemistry mechanisms in the model taken into account different chemical solvers, we select the photochemical mechanism CBM-Z because it affords a reasonable trade-off between accuracy and computational efficiency. During the prior work including the validation stages of the gas-phase schemes (results not shown) we used KPP to generate the Fortran code of three different gas-phase schemes CBM-Z (Zaveri and Peters, 1999), GEOS-CHEM (Evans et al. 2003) and the Regional Atmospheric Chemistry Model "RACM" (Stockwell et al.1997). In order to fit within our main aim of the chemical weather prediction, we didn't use both of GEOS-CHEM and RACM because they are very computationally expensive schemes due to their extensive number of chemical reactions. The KPP provides a flexible tool to generate a well coded chemical mechanism according to the user choice of a given ODE solver. We use KPP tools to create the gas-phase chemical mechanisms including the solvers for three chemical mechanisms. Usually, the Rosenbrock solver is selected for most of simulations due to its ability as a fast computational solver (Sandu et al 1997).

234 d) Photolysis Rates

235 Photolysis rates are determined as a function of various meteorological and conditional inputs. Rates for specific conditions
236 are determined by interpolating from an array of pre-determined values. The latter is based on the Tropospheric Ultraviolet-
237 Visible Model (TUV) developed by Madronich and Flocke (1999), using a pseudo-spherical discrete ordinates method
238 (Stamnes et al., 1988) with 8 streams. The 8-stream TUV is the most accurate method for determining photolysis rates but is
239 computationally too expensive for use in 3D models. Photolysis rate constants are calculated using the Fast-J radiative
240 transfer model (Wild et al., 2000) with O(1D) quantum yields updated to JPL2003 (Sander et al., 2003).

241 For simplicity, photolysis rates are estimated as the following. At first, for the simple reactions the photolysis rates are
242 estimated as a function of number of parameters such as meteorological and chemical inputs including altitude, solar zenith
243 angle, overhead column densities for O₃, SO₂ and NO₂, surface albedo, aerosol optical depth, aerosol single scattering albedo,
244 cloud optical depth and cloud altitude. At second, for the complex reactions, the photolysis rates are estimated as lookup table
245 using the TUV model. TUV is run offline and calculated a lookup table of the photolysis rates, and then this lookup table is
246 implemented under different weather conditions inside the model.

247 Photolysis rates can be significantly affected by the presence of clouds. Cloud optical depths are determined using the
248 random overlap treatment described by Feng et al. (2004), which assumes that cloudy and cloud-free sub-regions in each
249 model grid box randomly overlap with cloudy and cloud-free sub-regions in grid boxes located above or below (Briegleb,
250 1992). The method used to correct for cloud cover is based on Chang et al. (1987), which requires information on cloud
251 optical depth for each model grid cell. Optical depth is used to reduce photolysis rates for layers within or below clouds to
252 account for UV attenuation or to increase photolysis rates due to above-cloud scattering. In general, below cloud photolysis
253 rates will be lower than the clear sky value due to the reduced transmission of radiation through the cloud. Similarly,
254 photolysis rates are enhanced above the cloud due to the reflected radiation from the cloud. Cloud optical depths and cloud
255 altitudes from Enviro-HIRLAM are used in the photolysis calculations, thereby directly coupling the photolysis rates and
256 chemical reactions to meteorological conditions at each model time step.

257 e) Heterogeneous chemistry

258 Many gas-phase species are water soluble and sulphate and ammonia together with water take part in binary/ternary
259 nucleation. In order to consider these processes, a simplified liquid-phase equilibrium mechanism with the most basic
260 equilibria is included in NWP-Chem-Liquid. The “NWP-Chem-Liquid” is a thermodynamic equilibrium model, described in
261 Korsholm et al. (2008). This equilibrium module is solved using the analytical equilibrium iteration method (Jacobson,
262 1999). The reactions are summarized in Korsholm (2009) and the module will be updated to include the impact of organic
263 compounds from anthropogenic and biogenic sources.

264 **2.4. Aerosol formation, dynamics and deposition**

265 a) Aerosol dynamics module

266 The first aerosol module in Enviro-HIRLAM was based on the CAC (Chemistry-Aerosol-Cloud) model with the modal
267 approach for description of aerosol size distribution (Baklanov, 2003; Gross and Baklanov, 2004) and considered only sulfur-
268 type aerosols (Korsholm, 2009).

269 The current version of the Enviro-HIRLAM model has M7 aerosol microphysics module (Vignati et al., 2004) together with
270 aerosol removal processes ported from ECHAM5-HAM climate model (Stier et al., 2005). There are two types of particles
271 considered: insoluble and mixed (water-soluble) particles. The particles are split into seven classes depending on particle size
272 and solubility by means of “pseudomodal” approach. Four classes are used to represent mixed particles, i.e., nucleation,
273 Aitken, accumulation, and coarse modes, and another three classes are for the insoluble (Aitken, accumulation, and coarse
274 modes). Four predominant aerosol types are included - black carbon (BC) and primary organic carbon (OC), sulfate, mineral
275 dust and sea salt. The M7 aerosol dynamics includes nucleation, coagulation, and sulfuric acid condensation processes.
276 Coagulation and condensation lead to formation of mixed particles from the insoluble ones. Different aerosol types
277 mentioned in above (as well as others, e.g. pollen particles) are provided as separate species in the model outputs along with
278 lumped PM₁₀ and PM_{2.5}.

279 b) Dry-deposition and Sedimentation

280 The dry deposition fluxes of gases and aerosols (for both number and mass concentrations) are calculated from the
281 aerodynamic, quasi-laminar boundary layer as the product of the surface layer concentration and the dry deposition velocity
282 (Stier et al., 2005). The fluxes are used as the lower boundary condition in the semi-implicit vertical diffusion TKE-CBR
283 scheme (Cuxart et al., 2000). The calculation of the dry deposition velocities is performed by means of serial resistance
284 approach. And the “big-leaf” method is used to calculate surface resistance (Ganzeveld and Lelieveld, 1995; Ganzeveld et al.,
285 1998) per each grid-cell for the snow/ice, water, bare soil, low-vegetation and forest surface types. The SO₂ soil resistance is
286 a function of soil pH, relative humidity, surface temperature, and the canopy resistance, while surface resistances for other
287 gases are prescribed. The canopy resistance is computed from stomatal resistance and monthly mean Leaf Area Index (LAI)
288 values from the Enviro-HIRLAM Interaction-Soil-Biosphere-Atmosphere scheme (Noilhan and Planton, 1989).

289 The sedimentation of the aerosol particles is calculated throughout the atmospheric column. The calculation of the
290 sedimentation velocity is based on the Stokes velocity with the Cunningham slip-flow correction factor accounting for non-
291 continuum effects (Seinfeld and Pandis, 2006). In order to satisfy the Courant-Friedrich-Lewy stability criterion, the
292 sedimentation velocity is limited by ratio of the model layer thickness and the time-step.

293 c) Wet-deposition

299 There are several options for the wet deposition in the model. The first version used the aerosol size dependent
300 parameterisation of Baklanov and Sørensen (2001). In the latest version fixed size- and composition-dependent scavenging
301 parameters are also applied for wet deposition calculation and are different for stratiform and convective clouds (Stier et al.,
302 2005). They were derived from measurements of interstitial and in-cloud aerosol contents. These scavenging coefficients
303 depend on the aerosol modes, total cloud water and fraction (liquid- and ice), and the conversion rates of cloud liquid water
304 and cloud ice to precipitation through auto-conversion, aggregation, and accretion processes. The precipitation re-evaporation
305 before it reaches the ground is also included. The STRACO cloud scheme (Sass, 2002) provides water- and ice- precipitation
306 fluxes, normalized by the precipitation rates, to wet-deposition scheme, which uses prescribed size-dependent collection
307 efficiencies for rain and snow (Seinfeld and Pandis, 1998).
308

309 *2.5. Emission modules and pre-processor*

310
311 The model includes anthropogenic, biomass burning (wildfires) and natural emission fluxes of both gases and aerosols. These
312 emissions are processed in different ways; because some of them are pure datasets derived from ground-based and satellite
313 observations. The others are interactively developing during the model integration and depend on the meteorological
314 conditions at current time-step and land-use, -cover or water surfaces types. The anthropogenic emission inventory developed
315 by TNO (Kuenen et al., 2014) and linked to the model is a dataset of yearly-accumulated fluxes of gases, such as CO, CH₄,
316 NO_x, SO₂, NH₃, Non-Methane Volatile Organic Compounds (NMVOC), and particulate matter (PM) in two size bins – 2.5
317 μm and 10 μm, which are attributed to 10 source-sectors, e.g., energy industries, residential combustion, industry, etc.,
318 denoted by SNAP (Selected Nomenclature for sources of Air Pollution) codes. The inventory has resolution of 0.06° x 0.12°
319 and covers the entire Europe, European part of Russia, North of Sahara and a part of Middle East. Total NMVOC emissions
320 are split into 25 VOC compound groups by source-sectors by country (Kuenen et al., 2010). The PM_{2.5}, PM₁₀ emissions
321 splitting into 6 aerosol species (BC, OC, Na, SO₄, Coarse Other Primary and Fine Other Primary particles) is applied
322 following TNO recommendation (Kuenen et al., 2010). Because the dataset contains accumulated surface fluxes, one needs
323 to redistribute them in order to reproduce diurnal, weekly and monthly emissions variability. The emissions can also occur at
324 different heights, e.g., emissions from power plants are elevated and from traffic are at the surface; so, vertical redistribution
325 is applied within first 8 model hybrid levels. Therefore, temporal and vertical profiles developed by TNO for different
326 gaseous and aerosol species and SNAP codes are used in the emission pre-processor. The global biomass burning (wildfires)
327 so-called the IS4FIRES (Sofiev et al., 2012) emission inventory developed by FMI has similar structure except a number and
328 kinds of available gaseous and aerosol species as well as the resolution. The inventory data is total PM flux. The flux is split
329 into PM_{2.5} and coarse PM consisting of ash. The PM_{2.5} primarily consists of Organic and Black Carbon (OC and BC) and a
330 remainder of organic matter that is not carbon; for details see (Andreae and Merlet, 2001). The biomass burning emissions
331 typically show a diurnal cycle variability, and therefore, corresponding coefficients are applied (Giglio, 2007). The wildfires
332 emissions are also redistributed vertically having different proportions in lowest 200 m and the highest up to 1 km over the
333 ground.

334 The natural emissions of gases and aerosols are fully interactive and calculated online. There is dimethyl sulfide (DMS;
335 Nightingale et al., 2000) emission from oceans, which depends on the wind speed and seasonal variability of DMS solution in
336 the water. Soluble sea-salt aerosol emissions (Zakey et al., 2008) are driven by wind speed and temperature and insoluble
337 mineral dust aerosol emissions (Zakey et al., 2006) also depend on meteorology as well as hydrological parameters. Both sea-
338 salt and dust aerosols are emitted in accumulation and coarse modes.
339

340 *2.6. Aerosol feedback mechanisms*

341 *a) Direct and semi-direct effects*

342
343 Enviro-HIRLAM contains parameterisations of the direct and semi-direct effects of aerosols. Direct and semi-direct effects
344 are realised by modification of the Savijärvi radiation scheme (Savijärvi, 1990; Wyser et al. 1999) with implementation of a
345 new fast analytical SW and LW aerosol transmittances, reflectances and absorptances. The 2-stream approximation equations
346 for anisotropic non-conservative scattering described by Thomas and Stamnes (2002) are used for these calculations. The
347 GADS/OPAC aerosols of Köpke et al. (1997) are used as input to the routine. The species include BC (soot), minerals
348 (nucleus, accumulation, coarse and transported modes), sulphuric acid, sea salt (accumulation and coarse modes), “water
349 soluble”, and “water insoluble” aerosols. In addition to the more standard nucleation, accumulation and coarse aerosol size
350 modes we consider, according to Köpke et al. (1997), the transported size mode to describe aerosols that have been
351 transported over a long distance, for instance Saharan aerosols that have been blown to the Atlantic ocean. In order to make
352 the calculations fast, optical properties that are spectrally averaged over the entire SW and LW spectra are used. The spectra
353 used are shown in Figure 4. The short wave spectrum is a clear sky spectrum from 2 km height in a standard atmosphere
354 (Anderson et al. 1986) calculated with the DISORT algorithm (Stamnes et al. 1988) run in the LibRadtran framework (Mayer
355 and Kylling 2005). The long wave spectrum is calculated similarly and is based on the overall atmospheric LW transmittance
356 of a standard atmosphere.
357

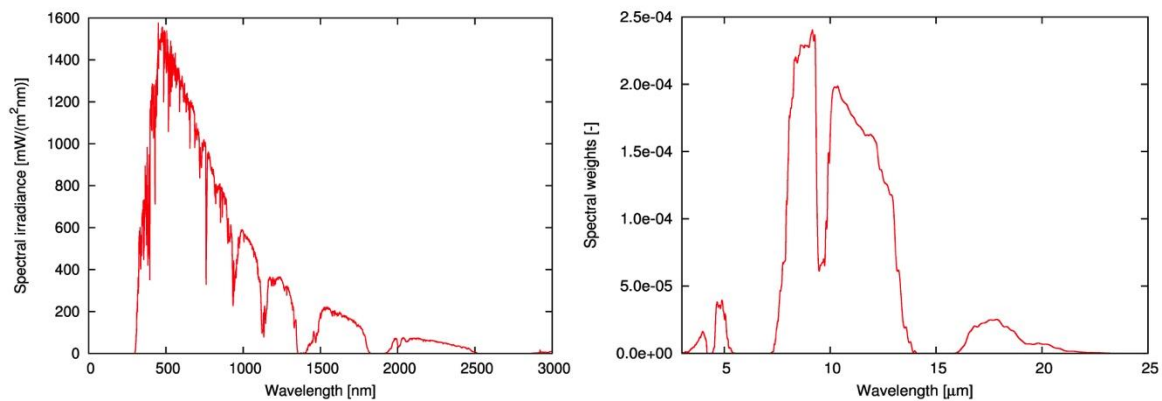


Figure 4: Left: The typical SW spectrum used for calculating average SW aerosol optical properties. Right: the spectral weights used for calculating average LW aerosol optical properties.

b) First and second indirect effects

For cloud-aerosol interactions a modified version of the Soft TRAnSition COndensation (STRACO) cloud scheme (Sass, 2002) is used in Enviro-HIRLAM. This scheme developed for operational NWP has recently been upgraded using new efficient methods to account for aerosol effects on cloud formation and microphysics. The scheme is able to account for convective transports of new variables. The prognostic aerosol fields are coupled directly to the cloud physical and microphysical properties. Liquid cloud droplet number is calculated based on aerosol size, number and solubility and the STRACO subgrid super saturation field is used as basis for the droplet nucleation calculation. This ensures consistency with the cloud water mass.

The modelled liquid droplet number evolves in time according to the following processes: droplet nucleation, self-collection, sedimentation and evaporation. In order to close the tendency calculations the liquid cloud droplet distribution is assumed to follow a gamma distribution where the shape parameter is calculated online using Geoffroy et al. (2010). Several schemes have been implemented for nucleation comprising Twomey (1959), Cohard et al. (1998), Cohard et al. (2000) and Abdul-Razzak et al. (1998), Abdul-Razzak and Ghan (2000). Self-collection is the process whereby droplets collide and stick together, but do not become rain-drops. The parameterization of self-collection processes follow Seifert and Beheng (2006). Sedimentation is calculated to be consistent with the mass of rain water in a given model time step under the basic assumption that the largest droplets are removed first from the cloud. Similarly, evaporation of a droplet below activation radius is calculated to be consistent with the total evaporated cloud water under the assumption that the smallest droplets evaporate first.

Cloud droplet effective radius controls the liquid phase absorptivity and transmissivity and is calculated from liquid water mass and droplet number and is here also dependent on the shape of the droplet distribution which evolves in time. Autoconversion follows Rasch and Kristjansson (1998), and is directly dependent on the calculated droplet number.

Abdul-Razzak and Ghan (2000) parameterization for aerosol activation has been extensively tested in many online-coupled weather and climate models. However, the STRACO cloud microphysics scheme with parameterizations of aerosol activation, cloud droplets nucleation, sedimentation, evaporation, self-collection, has been evaluated only with 1D column HIRLAM, so it needs to be further thoroughly evaluated.

2.7. Urban parameterisations and models urbanisation

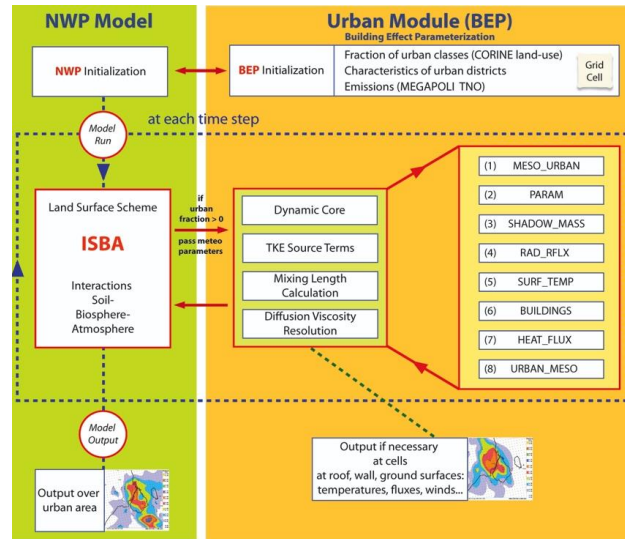
The representation of urban areas in Enviro-HIRLAM contains the following aspects and processes (Baklanov et al., 2005):

(i) model down-scaling, including increasing vertical and horizontal resolution and nesting techniques; (ii) modified high-resolution urban land-use classifications, parameterizations and algorithms for roughness parameters in urban areas based on the morphologic method; (iii) specific parameterization of the urban fluxes in the meso-scale model; (iv) modelling/parameterization of meteorological fields in the urban sublayer; (v) calculation of the urban mixing height based on prognostic approaches.

The nesting technics and downscaling methods are actively and successfully used for urban areas to reach the necessary resolution for resolving or parameterisation of urban features and effects. The details of this approach with the Enviro-HIRLAM model were described e.g. in Baklanov and Nuterman (2009). With respect to metropolitan areas, the downscaling for finer resolution allows to reproduce smaller scale meteorological patterns, and then these patterns are further modified through running urban parameterization modules only for grid cells where the cities are presented.

The urban parameterizations in the model contain three different approaches which may be combined. The first - simplest implementation contains modifications of the surface roughness, the anthropogenic heat flux, the storage heat flux and the albedo over urban areas. These are identified in the model using urban fractions extracted from the land-use database (CORINE) employed at DMI (Mahura et al., 2005b, 2006a, 2007a; Baklanov et al., 2005, 2008). The first module is the computationally cheapest way of "urbanising" the model and it can be used for operational NWP as well as for regional climate modelling. The second – Building Effect Parameterization (BEP) (Martilli et al., 2002) – module gives a possibility to consider the energy budget components and fluxes inside the urban canopy although it is a relatively more expensive (5–

410 10% computational time increase) (Mahura et al., 2008bc; 2010b; Figure 5). However, this approach is sensitive to the
 411 vertical resolution of NWP models and is not very effective if the first model level is higher than 30 m. Therefore, the
 412 increasing of the vertical resolution of current NWP models is required. The third – Soil Model for SubMeso Urbanized
 413 (SM2-U) version (Dupont and Mestayer, 2006; Dupont et al., 2006) – module is considerably more expensive
 414 computationally than the first two modules (Mahura et al., 2005a; Baklanov et al., 2008b). However, the third one provides
 415 the possibility to accurately study the urban soil and canopy energy exchange including the water budget. Therefore, the BEP
 416 scheme is considered as the baseline option and third SM2-U module is recommended only for use in advanced urban-scale
 417 NWP and meso-meteorological research models. The details of implementations of different urban modules, own
 418 developments and comparisons of different approaches and modules were published in previous papers (Mahura et al.,
 419 2005ab; 2006a; 2008abc; 2010b; Baklanov et al., 2005, 2008b). The main approach includes an integration of the urban
 420 modules into the ISBA (Interaction Soil- Biosphere- Atmosphere) land surface scheme of the NWP / HIRLAM model. The
 421 urban modules are activated only on those grid cells of the model domain where the urban fraction is presented.
 422



423
 424
 425 **Figure 5:** General scheme of the Building Effect Parameterisation (BEP) module for the Enviro-HIRLAM model
 426 urbanization with a structure of the subroutine conception (adapted from Mahura et al., 2010b).
 427

428 The urban boundary layer is very inhomogeneous and plays an important role in forming urban meteorological fields and
 429 especially in dispersion of atmospheric pollutants, Therefore, for calculation of the urban mixing height, additionally to the
 430 common diagnostic approaches, prognostic equations were used according to Zilitinkevich et al. (2002) and Zilitinkevich and
 431 Baklanov (2002).
 432

433 2.8. Transport schemes

434
 435 Until 2012 there were basically two options for transport schemes in Enviro-HIRLAM (Chenevez et al., 2004): a) the
 436 traditional non-conserving but highly efficient semi-Lagrangian (SL) scheme (Robert, 1981) in HIRLAM, b) the much less
 437 efficient flux based and positive definite finite volume scheme by Bott (1989) with updates by Easter (1993). In 2012 the
 438 default transport scheme was updated to a new monotonic version of the locally mass conserving semi-Lagrangian (LMCSL)
 439 scheme (Kaas 2008, Sørensen et al. 2013). This scheme, used in the present version of Enviro-HIRLAM, to be described
 440 briefly below is almost as efficient as the traditional SL scheme but now with the attractive properties of inherent mass
 441 conservation, plus being monotonic and positive definite.

442 In HIRLAM and former versions of Enviro-HIRLAM a traditional SL scheme is used for advecting the specific
 443 concentration of water constituents or the mixing ratio q_i of any tracer i . Considering mixing ratio this means that when
 444 ignoring any sources/sinks and turbulent mixing the prognostic transport equation to be solved is simply

$$445 \frac{dq_i}{dt} = 0 \quad (1)$$

446 The traditional SL numerical integration of Eq (1) reads

$$447 (q_i)_k^{n+1} = (q_i)_{*k}^n \quad (2)$$

448 where subscript k is the grid point/cell index and superscripts n and $n+1$ represent two consecutive time steps, respectively.
 449 The subscript $*k$ indicates the tricubic interpolation to the location of the departure point of the upstream trajectory, which
 450 arrives in grid point k at time level $n+1$. The tricubic interpolation in (2) can also be represented as a sum of interpolation
 451 weights involving 64 grid points surrounding the departure point. Formally this can be expressed

$$452 (q_i)_k^{n+1} = \sum_{l=1}^K w_{k,l} (q_i)_l^n \quad (3)$$

453 where K is the total number of grid points in the entire integration domain. Note that for each k only 64 $w_{k,l}$ weights are
 454 different from zero. When converting mixing ratio into volume density, i.e., $(r_i)_k^{n+1} = (r_d)_k^{n+1} (q_i)_k^{n+1}$, and subsequently
 455 summing over the integration area the traditional SL scheme is not mass conserving. Therefore in LMCSL (Kaas, 2008) a
 456 different approach is followed, namely, as in most other mass conserving transport schemes, to solve the complete continuity
 457 equation

$$458 \quad \frac{\partial r_i}{\partial t} = -\nabla \cdot (r_i \mathbf{u}) \quad \text{or} \quad \frac{dr_i}{dt} = -r_i \nabla \cdot \mathbf{u} \quad (4)$$

459 still omitting sources/sinks and turbulent mixing and then evaluating the mixing ratio from $(q_i)_k^{n+1} = (r_i)_k^{n+1} / (r_d)_k^{n+1}$. In
 460 LMCSL (4) is solved in a rather unusual way by modifying the interpolation weights in (3) in such a way that the sum of
 461 mass given off at time step n by a Eulerian grid cell l to all departure points that it influences is exactly equal to its own mass.
 462 In other words LMCSL is based on simple partition of unity. The modified weights become:

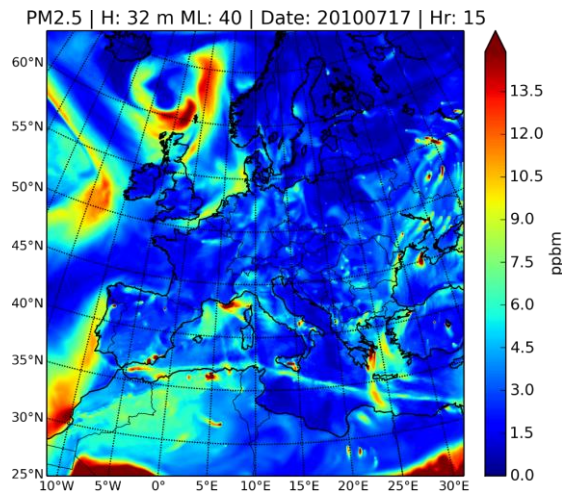
$$463 \quad \hat{w}_{k,l} = \frac{V_l}{V_k} \frac{w_{k,l}}{\sum_{m=1}^K w_{m,l}} \quad (5)$$

464 where V_k is the volume of Eulerian grid cell k . Using the modified weights the basic LMCSL forecast reads:

$$465 \quad (\rho_i)_k^{n+1} = \sum_{l=1}^K \hat{w}_{k,l} (\rho_i)_l^n \quad (6)$$

466 As the traditional SL scheme the LMCSL is not inherently monotonic or positive definite. Therefore an a posteriori iterative
 467 locally mass-conserving (ILMC) filter was developed, Sørensen et al. (2013). This filter ensures that the mixing ratio of the
 468 forecast will never be larger/smaller than the largest/smallest mixing ratio of the eight grid cells surrounding the upstream
 469 trajectory departure point at time level n . The ILMC filter designed to be as local as possible since non-local filters will
 470 generate non-physical chemical reactions. This is ensured by an iterative approach where the mass discrepancy is re-
 471 distributed among the neighbouring cells in the first iteration, and increasing the distribution radius, in case there is remaining
 472 mass discrepancy, for the next iteration(s). In general one or two iteration(s) are sufficient.

473 The LMCSL transport scheme in combination with the ILMC produces accurate monotonic and positive definite forecasts for
 474 water vapour, liquid/ice water and chemical constituents. As an example the simulated $\text{PM}_{2.5}$ concentration on July 17 in
 475 2010 with horizontal resolution of approximately 16 km's is shown in Figure 6. It can be seen that the model is able to
 476 reproduce, e.g., sharp transitions related to fronts over the North Atlantic. A more in depth analysis of the ability of ILMC to
 477 reproduce sharp gradients can be found in Sørensen et al. (2013), in particular Figure 3 and the accompanying discussion in
 478 that paper.



479
 480 **Figure 6:** Example of the simulated $\text{PM}_{2.5}$ concentration over Europe on July 17 in 2010 with horizontal resolution of 16 km.
 481

482 It should be noted that the dynamical core in Enviro-HIRLAM is identical to that of HIRLAM. Thus, the dry-air density for
 483 dynamics is calculated using a traditional SL approximation to (Eq. 4), i.e. not the LMCSL. Therefore, the Enviro-HIRLAM
 484 is not formally wind-mass consistent regarding tracer transport. However, the large scale precipitation fields in the traditional
 485 HIRLAM and Enviro-HIRLAM are very similar (see, e.g., Figure 4 in Sørensen et al. (2013)), which suggests that wind-mass
 486 inconsistency is of minor importance. In principle no monotonic transport schemes can be mass-wind consistent since the
 487 monotonic limiters formally destroy the consistency (see discussions on the issue of mass-wind inconsistency in atmospheric
 488 models in Jöckel et al. (2001)).
 489

490 3. Modelling system applications

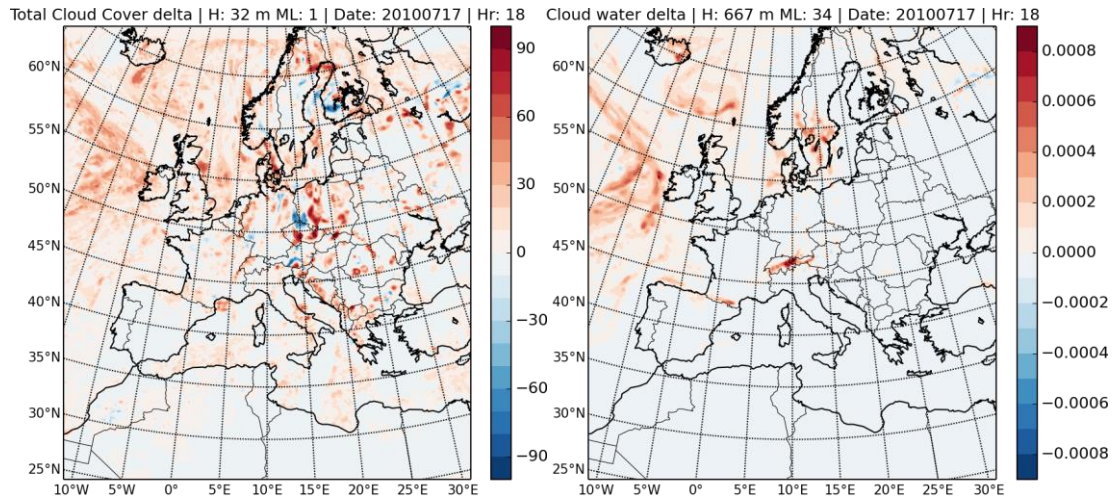
Possible applications of the online integrated Enviro-HIRLAM modelling system include the following: chemical weather forecasting, air quality and chemical composition longer-term assessment, weather forecast (e.g., in urban areas, severe weather events, etc.), pollen and bio-aerosols transport forecasting, climate change modelling, studies of climate change effects on atmospheric pollution on different scales, anthropogenic impacts on atmospheric processes, weather modifications, geo-engineering, contamination from volcano eruptions, sand and dust storms, nuclear explosion consequences, and other emergency preparedness modelling. Several realised/tested types of applications of the Enviro-HIRLAM for meteorological, environmental and climate forecasting and assessment studies are highlighted in Figure 1 and will be demonstrated below.

3.1. Applications for Numerical Weather Prediction

Several Enviro-HIRLAM sensitivity and validation studies of aerosol feedbacks on meteorological processes were done previously (see e.g., Korsholm, 2009; Korsholm et al., 2010; Baklanov et al., 2011ab; Sokhi et al., 2016). For example, the effects of urban aerosols on the urban boundary layer height, can be comparable with the effects of the urban heat island (Δh is up to 100–200m for stable boundary layer) (Baklanov et al., 2008a). Further studies (Korsholm et al., 2010) of megacities effects on the meteorology/climate and atmospheric composition showed that aerosol feedbacks through the first and second indirect effect induce considerable changes in meteorological fields and large changes in chemical composition (see Section 3.4), in a case of convective clouds and little precipitation. The monthly averaged changes in surface temperature due to aerosol indirect effects of primary aerosol emissions in Western Europe were analysed and validated vs. measurement data. It was found that a monthly averaged signal (difference between runs with and without the indirect effects) in surface temperature can reach 0.5°C (Figure 2.2b in Korsholm et al., 2010). Korsholm (2009) studied the impact of aerosol indirect effects on surface temperatures and air pollutant concentrations for a 24 h simulation over a domain in northern France including Paris in a convective case with low precipitation. He found a marginally improved agreement with observed 2m temperatures and a marked redistribution of NO₂ in the domain, primarily as a result of the second indirect effect.

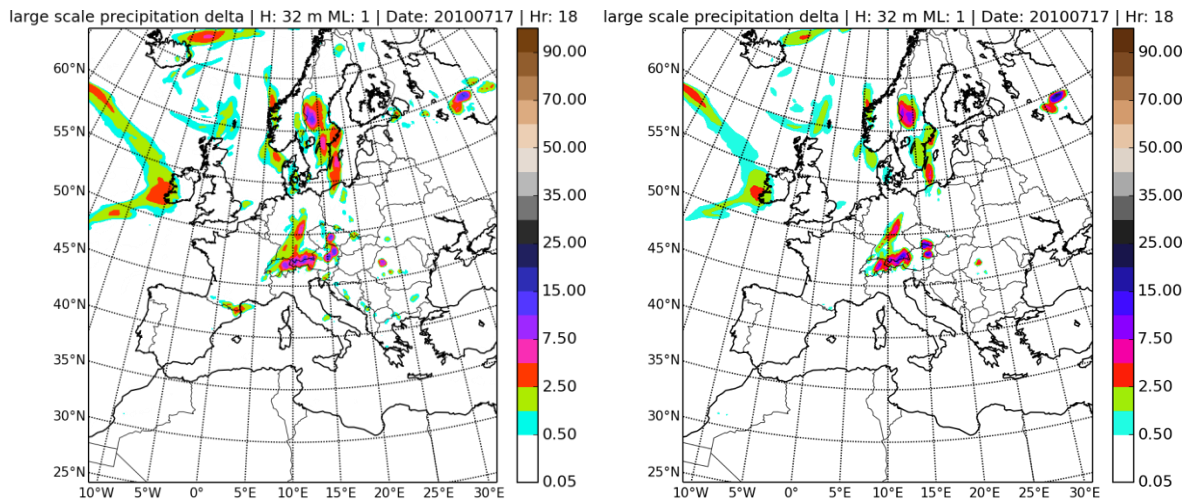
To perform analysis of atmospheric aerosol effects on clouds and precipitation, the year 2010 was selected for Enviro-HIRLAM simulations. That year, especially summer, was characterized by severe weather events such as floods, heat waves and droughts across Middle East, most of Europe and European Russia. The model was forced by boundary and initial conditions produced by ECMWF IFS (IFS-CY40r1) and MOZART (Horowitz et al., 2003) models for meteorology and atmospheric composition, respectively. The Enviro-HIRLAM modelling domain with horizontal resolution of 0.15° x 0.15° having 310 x 310 grid cells, and 40 vertical hybrid sigma levels extending to pressures less than 10 hPa, covers Europe, North of Sahara, and European Russia. The modelling domain was partitioned into 120 CPU cores and the model was run with time step of 300 seconds. The model includes emissions from anthropogenic sources developed by TNO and from wildfires produced by FMI as well as interactive DMS, sea-salt and dust emissions (for details see Sect. 2.5).

For aerosol-cloud interactions, these were estimated also for July 2010 by means of delta function, i.e., difference between outputs of models: Enviro-HIRLAM with aerosol-cloud interactions (ENV) and Reference-HIRLAM (REF). Fig. 7a shows deltas (ENV–REF) of total cloud cover over model domain, which is mainly increased (with local maxima up to 90%) except several inland areas, such as Finland, borders of Germany, Poland and Austria, where cloud cover decreased by almost 10 fold. The ENV runs revealed the increase of average cloud top height by approximately 2%. The delta function of cloud water content at average cloud base shows (Fig. 7b) its increase compared to REF and local maxima over North Atlantic, North Sea, Sweden, Switzerland, and Austria. These areas are occupied by precipitating clouds as seen in Fig. 8. The absolute frequencies of stratiform and convective precipitation over computational domain are decreased compared to the REF model, while the amount of convective precipitation during heavy precipitation events is increased. Hence, the wet deposition of particles decreases in summer because it rather depends on precipitation frequency than on its amount. The REF model run tends to over-predict both frequency and amount of precipitation. But the inclusion of aerosol-cloud interactions can improve general model performance, i.e., the ENV run bias for precipitation with respect to its frequency and amount has been decreased compared to the REF model run (Fig. 9).



(a) (b)
Figure 7: Delta (Enviro-HIRLAM – Reference-HIRLAM) of (a) vertically integrated total cloud cover [%] and (b) cloud water content [kg/kg] at average cloud base (667 m) on 17 Jul 2010, 18 UTC.

540
 541
 542
 543
 544
 545
 546



(a) (b)
Figure 8: Accumulated (3 hour) precipitation patterns from Reference-HIRLAM (REF) and Enviro-HIRLAM with aerosol-cloud interactions (ENV) on 17 Jul 2010, 18 UTC: stratiform precipitation: (a) – REF, (b) – ENV.

547
 548
 549
 550
 551
 552

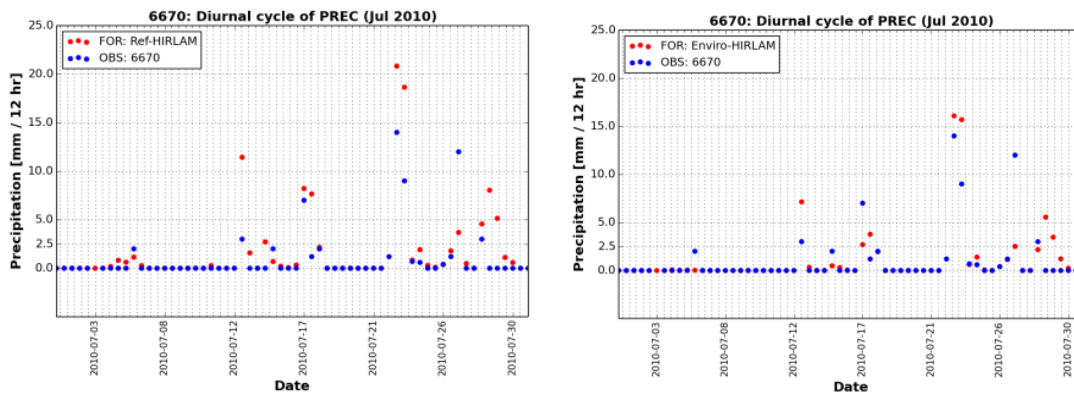


Figure 9: Precipitation amount (12 hours accumulated) of reference HIRLAM (left) and Enviro-HIRLAM with aerosol-cloud interactions (right) vs. surface synoptic observations at WMO station 6670 at Zurich, Switzerland (lat: 47.47; lon: 8.53) during Jul 2010.

553
 554
 555
 556
 557

Sensitivity studies on the model response to aerosol effects indicate strong “signals”, but it doesn't guaranty improvements. E.g., Korsholm (2009) considered evaluations only for some elements (e.g., the coupling interval) in the previous analysis and made corresponding conclusions about the improvements. Other feedback mechanisms, especially for aerosol-cloud interactions, were analysed mostly as sensitivity studies or evaluations for short-term episodes.

The model formulations have only been tested on a case basis and although strong signals have been found, this does not imply improved meteorological performance of the model. In particular, testing over longer periods including all seasons was not conducted that time. Furthermore, the interactions between aerosols and the cloud ice-phase are not in a state where improvements would be expected. Therefore, it is necessary to mention that it is too early to make conclusions about the improvement of precipitation forecasting by implementation of the indirect aerosol effects, because of large uncertainties in parameterisation of the cloud-aerosol microphysics processes (especially for ice-nucleation) and due to adjustments of such effects indirectly in NWP model parameters and constants (retuning of them after implementation of the aerosol feedbacks is needed). More investigations, further improvements and evaluations are needed for aerosol indirect effects and aerosol-cloud microphysics schemes in the model. Recently such evaluation studies are realised within the CarboNord project for monthly and annual validation studies and will be published separately.

3.2. Urban meteorology and environment prediction and assessments

The analysis of urban boundary layer (UBL) for metropolitan areas of megacity Paris (more than 10 mil population) and growing medium-size Bilbao (1 mil) placed over a semi-flat and coastal-complex terrains, respectively, was performed employing the Enviro-HIRLAM model. In particular, the 1) evaluation of the model performance coupled with urban module for different types of terrain and size of cities; and 2) estimation of urban heat island (UHI) development over selected urban areas and surroundings were done.

The Enviro-HIRLAM simulations were performed for nested domains with horizontal resolutions of 15, 5 and 2.5 km and for selected periods in July 2009. The meteorological boundary conditions were provided by the European Centre for Medium Range Weather Forecast (ECMWF) every 3 hour. The model was employed in 2 modes. The 1st mode is *control (CTRL)* run. The 2nd mode is *urban (URB)* run – e.g. coupled with the Building Effect Parameterization (BEP, Martilli et al., 2002) module and anthropogenic heat fluxes (AHF) from the Large scale Urban Consumption of energy (LUCY) model (Allen et al., 2010). Extracted AHFs were 60 and 40 W m⁻² for the Paris and Bilbao metropolitan areas, respectively. For the URB run at the finest resolution, the Paris and Bilbao urban areas were represented by 220 and 16 urban cells, respectively (Figure 10; adapted from González-Aparicio et al. 2010). In each grid-cell, BEP parameterizes the flux exchange between the urban surface and the atmosphere depending on combination of different urban districts, e.g. residential, low and high buildings, industrial and commercial.

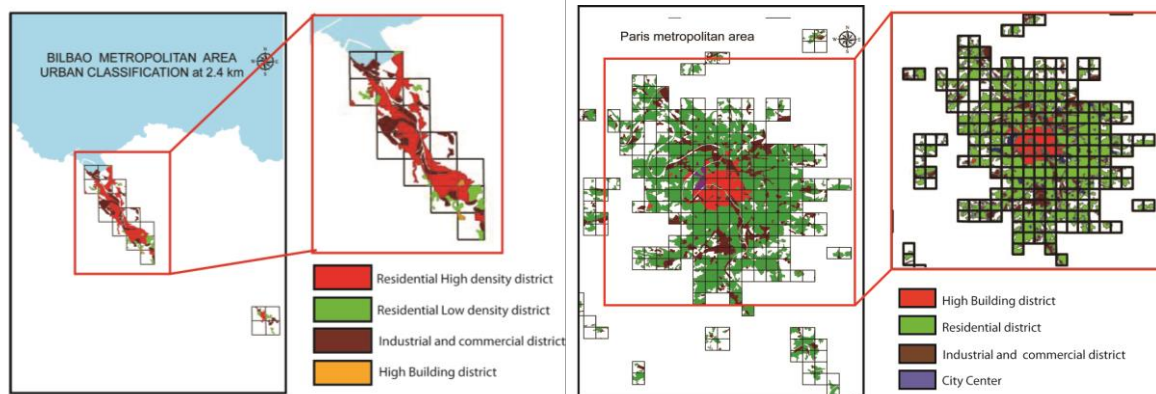


Figure 10: Urban district classification based on urban zoning data for the a) Bilbao and b) Paris metropolitan area, including the residential area (ReD), low and high building districts (LBD and HBD, respectively) and industrial and commercial districts (ICD). Spatial distribution of urban districts (HBD – high buildings, RD – residential, ICD – industrial commercial, and CC – city center districts) for the Paris metropolitan area within the P01 modelling domain (partly adopted from González-Aparicio et al. 2014).

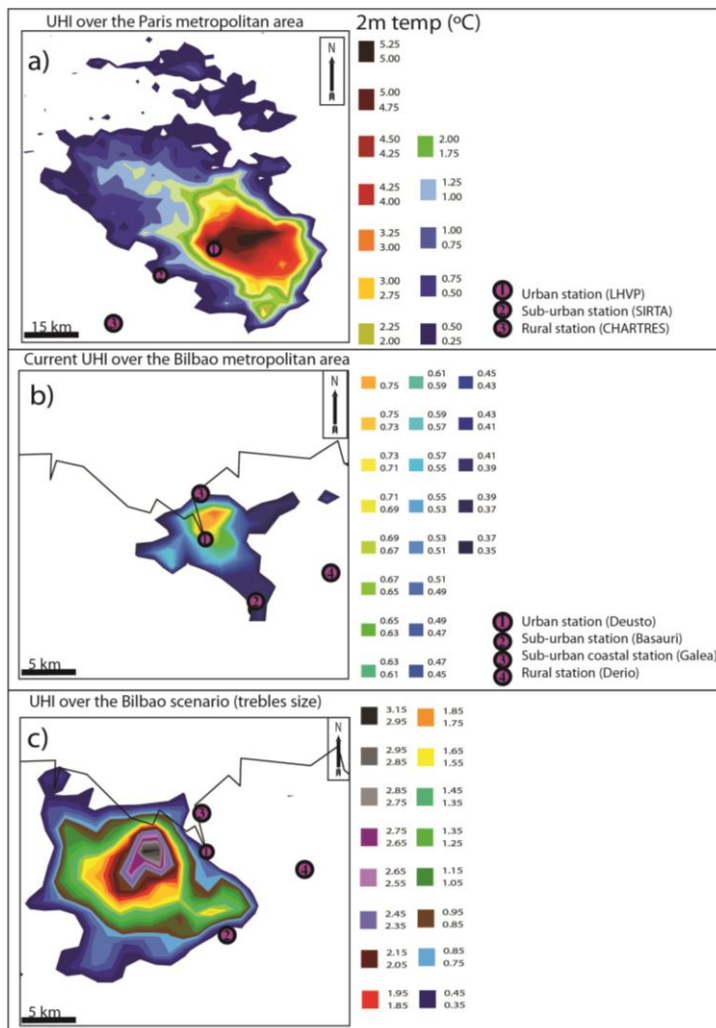
The statistical analysis showed that the urban simulation had a reduced bias with respect to observations than the control simulations. For Paris, on a monthly basis, the correlations for air temperature were higher for the URB compared to CTRL run, and results improved up to 10% on a diurnal cycle (with a maximum of 0.83 at 08 UTC). The correlations were slightly lower (down to 0.5) at early morning hours and slightly higher (up to 0.8) during afternoon and night-time. Moreover, correlations at suburban and urban stations were similar to correlations at rural stations (see Figure 11a). Analysis for Bilbao (González-Aparicio et al. 2013) showed similar performance of the model for both runs: with correlation for air temperature about 0.85 and 0.88 for summer and winter, respectively. For the specific humidity it was 0.75 and 0.92. For the wind speed, the highest value (0.8) is in summer, and during winter it decreased to 0.6 (0.4) near the coast (inland) stations.

608 The results of simulations for two selected cities showed that the model reproduced well the meso-scale processes at regional
609 scale, inland winds over Paris and land-sea breeze interactions over Bilbao. For selected locations (e.g. coastal vs. inland
610 sites), the bias between the observations and simulations was higher over Bilbao (maritime) than over Paris (continental)
611 cities. Although hydrostaticity of the model over a complex terrain is a limitation, but sensitivity test over Bilbao showed that
612 at 2.5 km optimal resolution it is possible at the same time to obtain satisfactory reproducibility of the large scale processes
613 and to explore the urban effects at finer scales.
614

615 The UHI development was also for short-term periods (here, for Paris – 28 Jul 2009; for Bilbao – 15 Jul 2009) with calm and
616 anticyclonic conditions. For Paris, three different locations were considered: urban (LHVP), suburban (SIRTA) and rural
617 (CHARTRES) stations (Figure 11a). As seen, the UHI was fully developed at 04 UTC with air temperature anomaly of 2.2°C
618 (LHVP) and 0.6°C (SIRTA). It started at mid-night and expanded covering area of about 2000 km². The heat island was
619 retained until 11 UTC, but during the daytime (e.g. 11-17 UTCs) the effect disappeared due to contribution of incoming solar
620 radiation. At CHARTRES this effect (0.2°C) was almost negligible. Both the wind speed and relative humidity were also
621 affected by the urban area: at LHVP the wind speed reduced by maximum 3.5 m s⁻¹ at 06 UTC, and the relative humidity -
622 down to 15% under developing UHI. At SIRTA the change in wind speed was down to 0.7 m s⁻¹ and at CHARTRES the
623 changes in wind speed and relative humidity were almost negligible.
624

625 For Bilbao, model showed that for breezes from northern directions, the impact of urban area on local flow dynamics is
626 inhibited; however, for breezes from southern directions - the urban effect had appeared. For example, on 15 Jul 2009, the
627 UHI was developed during night-morning hours (e.g. 23-09 UTCs) with maximum up to 1°C, and heat island expanded
628 covering area of about 130 km². In addition, González-Aparicio et al. (2013) showed that the UHI intensity is lower in winter
629 compared with summer, underlying that dominating factor is the surface heating during daytime, which is higher in summer
630 than in winter.
631

632 As medium size cities are under continuous development, future impacts of urbanization are expected to become more
633 significant. Several different scenarios of urban development were tested for Bilbao (González-Aparicio et al., 2014). Enviro-
634 HIRLAM model runs showed that under calm conditions during summer and winter, the UHI could reach up to 2.2°C
635 covering area of about 400 km² when city is doubled in size or doubled in AHF. When city is tripled in size, the UHI could
636 reach up to 3°C with urban island expansion up to 550 km² (Figure 11c). Analysis of UHI for Bilbao (e.g. triple size city
637 scenario) vs. current UHI over Paris showed similar intensity of up to 3°C, and UHI boundaries are different, e.g. for Paris it
638 was 4 times larger. Such differences can be explained by different cities' sizes, morphologies and characteristic AHFs.
639



640
641 **Figure 11:** Difference plots for the air temperature at 2m between outputs of the URB (urbanized -BEP + AHF-) and CTRL
642 (non-urbanized) Enviro-HIRLAM model under calm conditions during summer 2009 for the a) Paris metropolitan area and
643 for the Bilbao metropolitan area b) in its current size of the city and c) under a scenario tripling the size of the city.
644

645 3.3. Pollen forecasting

646
647 Among air-pollinated allergens, birch pollen is one of the most important for the population group suffering allergic diseases.
648 The number of allergic patients sensitive to birch pollen is assessed as 20% of European population (WHO, 2003; Linneberg,
649 2011) and this number is constantly increasing. In particular, in Denmark the number of allergic patients has increased twice
650 over the past few decades (Linneberg, 2011). These facts demonstrate the importance of operational birch pollen forecasting
651 for the European population especially during the spring season. Currently, birch pollen is presented as biological air
652 pollutant in different NWP and ACT models such as SILAM (Finland), COSMO-ART (Germany, Switzerland, Austria),
653 CHIMERE (France), Enviro-HIRLAM, DEHM (Denmark) and others. The pollen emissions are strongly dependent on
654 meteorology, so it is advantageous to simulate and forecast pollen pollution episodes by online-coupled meteorology-air
655 pollution models since all necessary meteorological fields are available at each model time step.

656 Original developments of the dynamical Enviro-HIRLAM based operational modelling system for the birch pollen
657 forecasting in Denmark (called Env-POLL) were started in 2006 (Rasmussen et al., 2006; Mahura et al., 2006b) including
658 previously developed statistical methods (Rasmussen, 2002), modelling of elevated concentrations episodes, analysis of
659 spatio-temporal and diurnal cycle variabilities, contribution of remote source regions into pollen levels, improvements in
660 emissions and parameterizations, etc. (Mahura et al., 2007b, 2009, 2010a). The most recent developments are shown in
661 Kurganskiy et al. (2015) with revised general scheme of input and output of the Enviro-HIRLAM birch pollen forecasting
662 system presented in Figure 12. The input includes the meteorological initial/ boundary conditions (IC/BC) obtained from the
663 IFS model system, birch forest fraction map, phenological data, i.e. temperature sum thresholds for start of flowering (Sofiev
664 et al., 2013), accumulated total number of birch pollen particles emitted from a unit area during the pollinating season.
665
666



Figure 12: General scheme of Enviro-HIRLAM birch pollen forecasting.

The forecasting of birch pollen concentrations requires information/data on the spatial birch tree distributions, characteristics of pollen release, its atmospheric transport and dispersion, its deposition due to gravitational settling and wet deposition, i.e. scavenging by precipitation. Birch pollen emissions are fully dependent on temporal and spatial variability of meteorological conditions. The emission module (Sofiev et al., 2013) includes the following parameters affecting the pollen release: 2-meter air temperature and relative humidity, 10-meter wind speed, and accumulated precipitation. The atmospheric transport is handled in the same way as for aerosols (see section 2.8). Dry deposition of birch pollen particles in the atmosphere is represented by gravitational settling (Seinfeld and Pandis, 2006) whereas dry deposition due-to interactions of particles with the surface can be neglected according to Sofiev et al., (2006). The wet deposition scheme distinguishes between in-cloud (Stier et al., 2005) and below-cloud scavenging (Baklanov and Sørensen, 2001). The output in terms of birch pollen forecasting, and for analysis, contains 2D fields of the birch pollen concentration at the lowest vertical model level. The modelling domain has 15 km horizontal resolution with 154 and 148 grid points along longitude and latitude, correspondingly. The domain covers the main European part and is centered around Denmark.

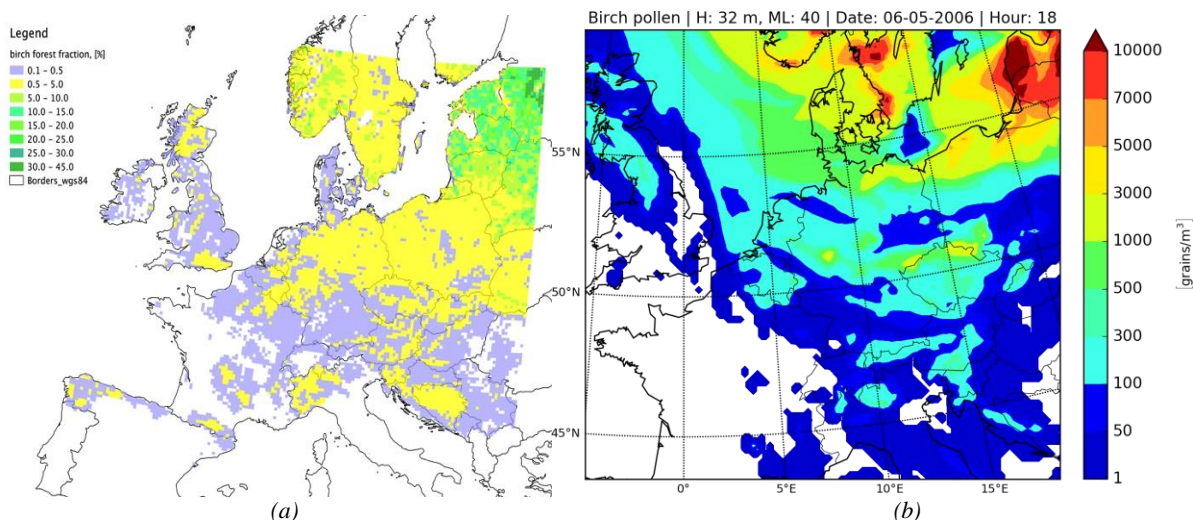


Figure 13: (a): Birch forest fraction map; (b): Example of the simulated birch pollen concentration in the modelling domain on the 6th of May, 2006 at 18 UTC.

Birch forest habitat map has been derived by GIS (Geographic Information System) analysis (<http://www.spatialanalysisonline.com>) for the selected modelling domain. The map (Fig. 13a) shows birch forest fraction in each model grid cell. Three GIS based databases were used in the derivation procedure: 1) Global Land Cover Characterisation (GLCC, <http://landcover.usgs.gov/glcc/>), 2) European Forest Institute (EFI, Päivinen et al., (2001)) and 3) Tree Species Inventory (TSI, Skjøth et al., (2008)). Both GLCC and EFI have 1 km horizontal resolution, whereas TSI has 50 km resolution.

As examples for the birch pollen season 2006 the model results were compared with observations for two Danish sites: Copenhagen and Viborg (Fig. 14). This year was dominated by a relatively cold spring over large areas of Europe followed by rapid warming and little/no rain. It caused short but intensive birch pollen season with long range transport episodes before the local flowering start and thereby emissions. The evaluation for both modelled and observed birch pollen concentrations showed extremely high values (daily averages about and even more than 1000 grains/m³) during 5-10 May 2006 episode for Copenhagen and 5-8 May 2006 episode for Viborg. The extremely high birch pollen concentrations over Denmark are also visible in Fig. 13b.

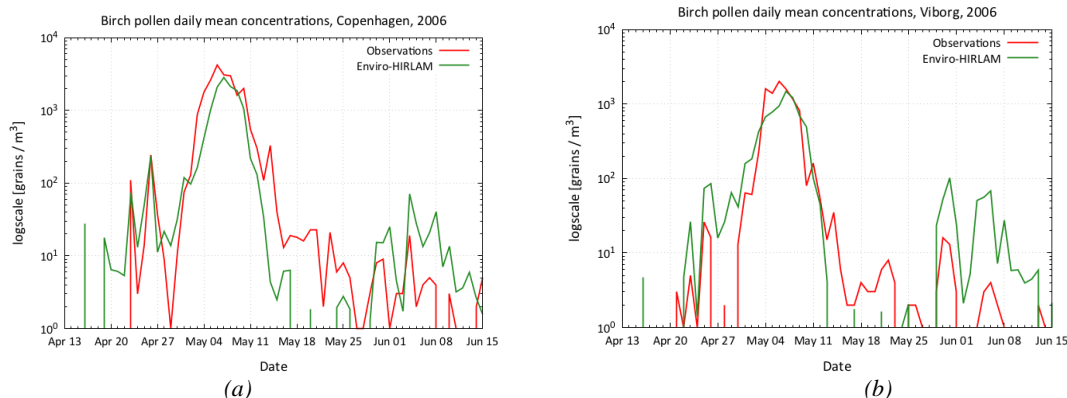


Figure 14: Birch pollen concentrations observed (red) vs. modelled (green) at Danish sites: Copenhagen (a) and Viborg (b).

According to Sofiev et al., (2011) and Siljamo et al. (2013) the following criteria can be used for assessment of birch pollen concentration forecasting: model accuracy (MA), hit rate (HR), false alarm ratio (FAR), probability of false detection (POFD) and odds ratio (OR). All of the criteria are calculated using four parameters obtained by assessment of the number of low and high modelled vs. observed birch pollen concentrations (C) relatively to a threshold value $N_{th} = 50 \text{ grains/m}^3$ (i.e. $C \geq N_{th}$ for high and $C < N_{th}$ for low-concentration days). The threshold has been chosen since most of the pollen allergy sensitive population might start suffering from allergic reactions when daily mean birch pollen concentration, $C \geq N_{th}$ in the air (Jantunen et al., 2012).

The results of statistical analysis showed high MA for both Danish stations (0.95 for Copenhagen and 0.84 for Viborg, 0.9 in average). Prediction of elevated/top concentrations (HR values) by the model was assessed as 0.93 for Copenhagen and 0.58 for Viborg. The FAR values indicated that the probability to get an incorrect top model concentration was 0.07 and 0.42 for Copenhagen and Viborg, respectively. The POFD criterion showed low probability to get high modelled concentrations for observed low-concentration days (0.02 for Copenhagen and 0.18 for Viborg). Finally, the OR indicated that the likelihood for getting “high” day concentration instead of a “low” (if the model prediction is “high”) were 42 and 3.26 times higher for Copenhagen and Viborg, respectively. In other words, the OR values show the ratio between HR and POFD. As it is seen from the OR values provided above, a fraction of the correct forecasts is prevailing for both Danish stations in this study.

It was found that comparing with observations, the modelled results reflected the general shape of changes in pollen concentration during the episode studied for both Danish stations: Copenhagen and Viborg. As it is also seen in Fig. 14 the model reproduces the magnitude of birch pollen concentrations for the peak period of the season in comparison with observations. However, some overestimation of the modelled concentration is visible for both stations at the end of the season. It can be explained by contribution due to long-range atmospheric transport of pollen from other remote regions, presumably from those located more northerly than Denmark and where the pollen season starts and ends later relatively to the Danish sites.

3.4. Chemical Weather Forecasting and air pollution applications

Validation and sensitivity tests (on examples of case studies and short-time episodes) of the online vs. off-line integrated versions of Enviro-HIRLAM (Korsholm et al., 2008) showed that the online coupling improved the results. Different parts of the model were evaluated vs. the ETEX-1 experiment, Chernobyl accident and Paris MEGAPOLI campaigns (summer 2009) datasets and showed that the model had performed reasonably well (Korsholm, 2009; Korsholm et al., 2009; 2010; Sokhi et al., 2017).

Online vs. off-line coupled simulations for the ETEX-1 release showed that the off-line coupling interval increase leads to considerable error and a false peak (not found in the observations), which almost disappears in the online version that resolves meso-scale influences during atmospheric transport and plume development (Korsholm et al., 2009). Further studies (Korsholm et al., 2010) of urban aerosol effects on the atmospheric composition showed that aerosol feedbacks through the first and second indirect effect induce large changes in chemical composition, in particular nitrogen dioxide, in a case of convective clouds and little precipitation. For the Paris campaign, on diurnal cycle variability the ozone concentration patterns showed dependencies on meteorological parameters, and especially seen at urban scale runs (Mahura et al., 2010b).

To perform further analysis of online coupling and feedback effects on atmospheric pollution forecasting, the year 2010 was selected (for details see Sect. 2.5). Nuterman et al. (2013) evaluated the Enviro-HIRLAM model for July 2010 vs. ground-based observations of $PM_{2.5}$ from EU AirBase air-quality network (Guerreiro et al., 2014), with a number of stations located in Denmark, Sweden, Germany and Spain (see Fig. 15a). The model runs were performed for the entire July 2010 with 7 days spin-up in June. Fig. 15b shows correlation coefficients on a diurnal cycle for $PM_{2.5}$ concentrations at selected measurement sites. In general it shows a fairly good positive correlations (more than +0.3), except for several Spanish stations (such as ES1938A at daytime, and ES1974A - at nighttime).

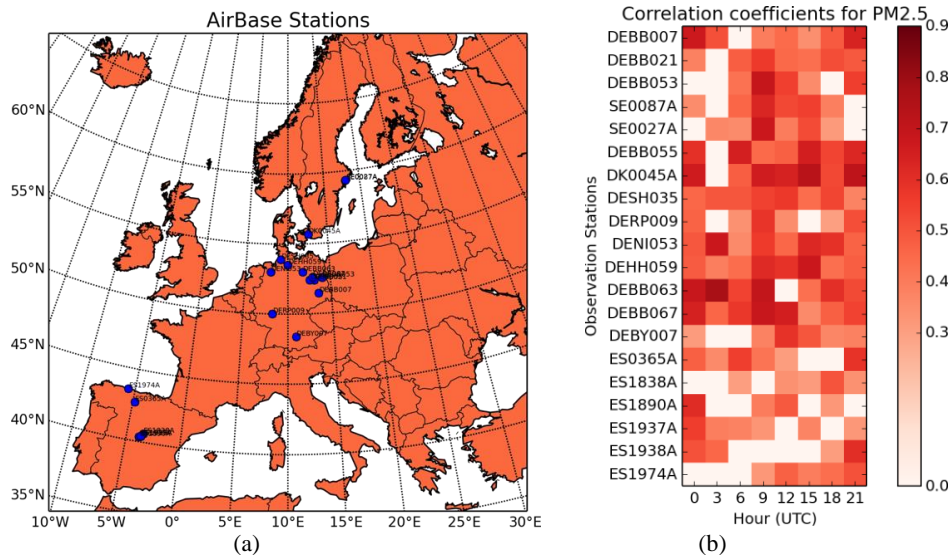


Figure 15: (a) Map of selected AirBase air-quality monitoring stations (<http://acm.eionet.europa.eu/databases/airbase/>) across Europe; (b) PM_{2.5} correlation coefficient on diurnal cycle for selected AirBase observation stations.

On the monthly based evaluation the model predicts well PM_{2.5} day-to-day variability, but always has negative bias (Fig. 16). This under-prediction is due to several reasons: i) aerosol microphysics without secondary organic aerosols; ii) lack of partitioning of ammonium nitrate; iii) rough model resolution, which still cannot capture small-scale effects like complex orography and urbanized regions (in particular, due to lack of fine-resolution emissions from anthropogenic sources, like urban traffic). For instance, the model shows negative bias of PM_{2.5} during daytime at Danish urban station (Fig. 16a). It is apparently due to rough model resolution in the considered runs. It was also found that PM_{2.5} values are very influenced by changes in atmospheric stability conditions, which difficult to predict accurately in many NWP models. This can be observed from correlation coefficient decrease at stations during night-time (at 03 UTC) or from underestimation of elevated concentrations. In spite of these issues, the model can well reproduce diurnal cycle of aerosols at different sites, e.g. urban (Fig. 16a), coastal and rural (Fig. 16b), and shows good overall performance.

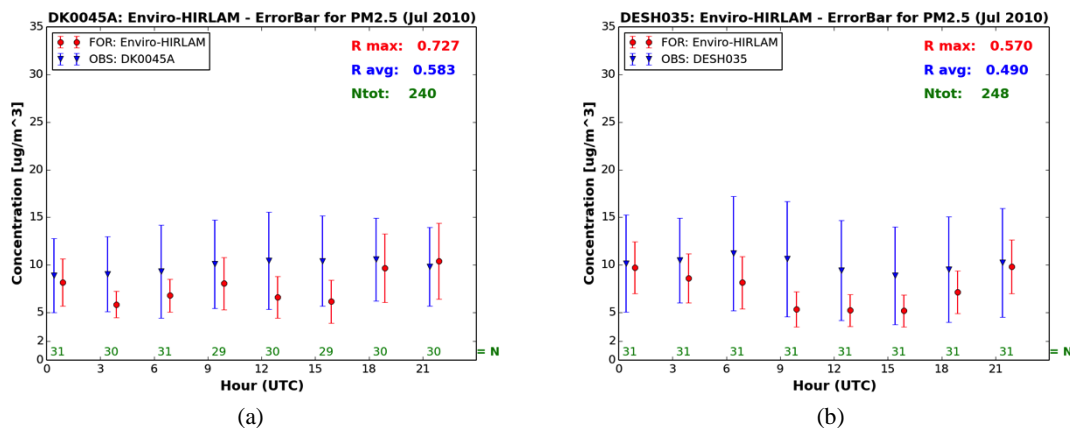


Figure 16: Error-bar concentrations [$\mu\text{g}/\text{m}^3$] on diurnal cycle for AirBase observations vs. Enviro-HIRLAM modelling results; (a) Danish urban station and (b) German rural station; Right top corner indicates maximum and average correlation coefficients for the station as well as total number of analysed observation samples; Green numbers along X axis indicate number of observation samples per time slice.

Further on-going developments of the Enviro-HIRLAM modelling system for atmospheric composition applications are realised within the FP7 MarcoPolo and NordForsk CarboNord projects. The Enviro-HIRLAM downscaling from regional-to-urban scale modelling is realised in MarcoPolo for the East China region and largest metropolitan agglomerations in China (Mahura et al., 2016) with a focus on providing services on meteorology and atmospheric composition (with focus on aerosols). The Northern Hemispheric low resolution modelling in a long-term mode is realized in CarboNord with focus on evaluation of black carbon as well as higher resolution modelling over European domain in a short-term mode with focus on feedbacks mechanisms evaluation (Nuterman et al., 2015; Kurganskiy et al., 2016).

4. Further discussions

785 Several types of the above described and previously published applications of the Enviro-HIRLAM for meteorological,
786 environmental and climate forecasting and assessment studies were tested and demonstrated. Different applications of
787 Enviro-HIRLAM (with downscaling from hemispheric - regional – subregional – urban scales) were realised for different
788 geographical regions and countries including European countries such as Denmark, Lithuania, France, Spain, Ukraine,
789 Russia, The Netherlands, Turkey and well as for other – Kazakhstan, China and Arctic regions.

790 It is clear that the seamless/ online integrated modelling approach realised in Enviro-HIRLAM is a perspective and state-of-
791 the-art way for future single-atmosphere modelling systems, providing advantages for all three communities: meteorological
792 modelling including NWP, AQ modelling including CWF, and climate modelling.

793 However, there is no necessarily one configuration of the integrated online modelling approach/ system suitable for all
794 communities, and that should be further investigated with practical needs for areas applications, approaches to coupling and
795 computing resources usage. In particular, based on previous studies and above shown examples the following could be
796 recommended for the considered applications:

- 797 • For AQ: online coupling improves air quality forecasts, and especially with full chemistry and aerosol feedbacks effects
798 included.
- 799 • For NWP: gas chemistry is not critical and can be simplified (or omitted), but aerosol feedbacks are important for
800 radiation and precipitation, and especially, for heavy polluted episodes and in urban areas.
- 801 • For pollen forecast: online coupling improves pollen emission parameterization and correspondingly modelling of
802 concentration and deposition; however, the feedbacks are not so important; the chemistry is not considered yet, but
803 interaction with allergens would be interesting to study in future (not done yet).
- 804 • For climate studies: it is suitable only for understanding the feedback mechanisms, but too expensive computationally
805 for climate time-scale runs (the model had been used usually for one year period runs); chemistry is important, there is a
806 need to be optimised and simplified.

807 It should also be mentioned that the considered evaluations of Enviro-HIRLAM were done only for some elements (e.g., the
808 coupling interval) in the previous analysis and main conclusions about the improvements were provided just for these. Other
809 feedback mechanisms, and especially for aerosol-cloud interactions, were analysed mostly as sensitivity studies or evaluated
810 for short-term episodes. In particular, the STRACO cloud scheme contains fairly simplified cloud microphysics (heavily
811 parameterized). Hence, tuning is essential for the overall performance of the model, when it comes to precipitation and cloud
812 physical properties.

813 5. Conclusions

814 In this manuscript we have provided a comprehensive description of the Environment – High Resolution Limited Area
815 Model (Enviro-HIRLAM), which is developed as a fully online coupled/ integrated numerical weather prediction and
816 atmospheric chemical transport modelling system for research and forecasting of joint meteorological, chemical and
817 biological weather.

818 Possible applications of the modelling system can include: chemical weather forecasting, air quality and chemical
819 composition for short- and long-term impact assessments on population and environment, multi-scale weather forecasting
820 (e.g., on regional and subregional scales, in urban areas, severe weather events, etc.), pollen and road weather conditions
821 forecasting, climate change forcing modelling, studies of climate change effects on atmospheric pollution on different scales,
822 weather modification and geoengineering methods, forest fires and volcano eruptions, dust storms, nuclear explosion
823 consequences, other emergency preparedness modelling.

824 Comprehensive online modelling systems, like Enviro-HIRLAM, built originally for research purposes and including all
825 important mechanisms of interactions, will help to understand the importance of different physical-chemical processes and
826 interactions and to create specific model configurations that are tailored for their respective purposes.

827 Multiple episode studies with the Enviro-HIRLAM model demonstrated the importance of including the meteorology and
828 chemistry (especially aerosols) interactions in online-coupled models. However, there is no one unique integrated online
829 modelling system configuration, which is the best suitable for all communities.

830 Highlighting a number of previous investigations we show that Enviro-HIRLAM has already been used for a host of different
831 applications ranging from pollen forecasting to numerical weather prediction.

832 It should be stressed that there are still main gaps remaining in understanding of several processes such as: (i) aerosol-cloud
833 interactions (still poorly represented); (ii) data assimilation in online models (still to be developed to avoid over-specification
834 and opposite cancelling effects); and (iii) model evaluation for online models needs more (process) data and long-term
835 measurements – and a test-bed.

836 Code and/or data availability

837 The Enviro-HIRLAM modelling system is a community model. The source code is available for non-commercial use (i.e.
838 research, development, and science education) upon agreement through contact with Bent Hansen Sass (bhs@dmi.dk) and
839 Roman Nuterman (nuterman@nbi.ku.dk). Documentation, educational materials and practical exercises are available from
840 <http://hirlam.org>, <http://hirlam.org/index.php/documentation/chemistry-branch> and YSSS training schools:
841 <http://neifam.fmi.fi/YSSS08>, <http://www.ysss.osenu.org.ua> and <http://aveirosummerschool2014.web.ua.pt>.

842 Acknowledgements:

847 This work was realised within and supported by the HIRLAM-A,-B,-C projects, COST Actions 715, 728 and ES1004
848 EuMetChem, and several European projects: EC FP5 ELCID, FUMAPEX, FP6 EnviroRISKS, FP7 MEGAPOLI,
849 TRANSPHORM, MACC, PEGASOS and MarcoPolo; NordForsk projects - NetFAM, MUSCATEN, CarboNord, CRAICC-
850 PEEX, CRUCIAL and others. Meteorological data were provided by the Paris measurement campaign of the FP7 EU
851 MEGAPOLI project and by the Basque Meteorological Agency (EUSKALMET). The authors are greatly thankful to the
852 colleagues involved into the model developments and applications at different stages: from the DMI team: J. Chenevez, A.
853 Gross, K. Lindberg, P. Lauritzen, C. Petersen, X. Yang, L. Laursen, J.H. Sørensen, B. Amstrup, and from collaborators teams
854 and PhD students: A. Mazeikis (Lithuania), S. Ivanov, Yu. Palamarchuk (Ukraine), S. Smyshlyayev, S. Mostamandy, E.
855 Morozova, Yu. GavriloVA, A. Suhodskiy, A. Penenko (Russia), H. Toros (Turkey), K. Bostanbekov (Kazakhstan), A. Stysiak
856 (Denmark). The authors are thankful to C. A. Skjøth (University of Worcester, UK) for providing the tree species inventory
857 (TSI) data; European Forest Institute (EFI) - for broadleaved forest data; Danish Asthma Allergy Association - for birch
858 pollen observation data; M. Sofiev and P. Siljamo (FMI, Helsinki) - for fruitful discussions of the birch pollen modelling
859 issues. The handling topical editor Dr. Jason Williams, as well as Prof. Nicolas Moussiopoulos and two anonymous
860 reviewers are thanked for thorough reviews, and for many valuable comments that substantially improved this article.

861 862 **References**

- 864 Abdul-Razzak, H. and Ghan, S. J.: A parameterization of aerosol activation: 2. Multiple aerosol types, *J. Geophys. Res.-*
865 *Atmos.*, 105, 6837–6844, doi:10.1029/1999JD901161, 2000.
- 866 Abdul-Razzak, H., Ghan, S. J., and Rivera-Carpio, C.: A parameterization of aerosol activation: 1. Single aerosol type, *J.*
867 *Geophys. Res.-Atmos.*, 103, 6123–6131, doi:10.1029/97JD03735, 1998.
- 868 Allen, L., Beevers, S., Lindberg, F., Iamarino, M., Kitiwiroon, N., and Grimmond, C.: Global to City Scale Urban
869 Anthropogenic Heat Flux: Model and Variability, MEGAPOLI Scientific Report, Tech. Rep. 10–01, King’s College
870 London, Environmental Monitoring and Modelling Group, London, 2010.
- 871 Anderson, G. P., Clough, S. A., Kneizys, F. X., Chetwynd, J. H., and Shettle, E. P.: AFGL Atmospheric Constituent
872 Profiles (0–120 km), Tech. Rep. AFGL-TR-86-0110, Air Force Geophysics Lab Hanscom AFB, MA, USA, 1986.
- 873 Andreae, M. O. and Merlet, P.: Emission of trace gases and aerosols from biomass burning, *Global Biogeochem.*
874 *Cy.*, 15, 955–966, doi:10.1029/2000GB001382, 2001.
- 875 Austin, J. and Butchart, N.: Coupled chemistry-climate model simulations for the period 1980 to 2020: Ozone depletion
876 and the start of ozone recovery, *Q. J. Roy. Meteor. Soc.*, 129, 3225–3249, doi:10.1256/qj.02.203, 2003.
- 877 Baklanov, A.: Numerical Modelling in Mine Aerodynamics, USSR Academy of Science, Apatity, 200 pp., 1988 (in
878 Russian).
- 879 Baklanov, A.: Modelling of formation and dynamics of radioactive aerosols in the atmosphere, in: *Research on a*
880 *Theory of Elementary Particles and Solid State*, 4, 135–148, 2003.
- 881 Baklanov, A.: Integrated meteorological and atmospheric chemical transport modeling: perspectives and strategy for
882 HIRLAM/HARMONIE, *HIRLAM Newsletter*, 53, 68–78, 2008.
- 883 Baklanov, A.: Chemical weather forecasting: a new concept of integrated modelling, *Adv. Sci. Res.*, 4, 23–27,
884 doi:10.5194/asr-4-23-2010, 2010.
- 885 Baklanov, A. and Korsholm, U.: On-line Integrated Meteorological and Chemical Transport Modelling: Advantages and
886 Prospectives, in: *Air Pollution Modeling and Its Application XIX*, edited by Borrego, C. and Miranda, A. I., Springer
887 Netherlands, Dordrecht, 3–17, doi:10.1007/978-1-4020-8453-9_1, 2008.
- 888 Baklanov, A. and Nutterman, R.: Multi-scale atmospheric environment modelling for urban areas, *Adv. Sci. Res.*, 3, 53–57,
889 2009.
- 890 Baklanov, A. and Sørensen, J.: Parameterisation of radionuclide deposition in atmospheric long-range transport
891 modelling, *Physics and Chemistry of the Earth, Part B: Hydrology, Oceans and Atmosphere*, 26, 787 – 799,
892 doi:10.1016/S1464-1909(01)00087-9, 2001.
- 893 Baklanov, A., Mahura, A., Nielsen, N., and Petersen, C.: Approaches for urbanization of DMI-HIRLAM NWP model,
894 *HIRLAM Newsletter*, 49, 61–75, December 2005.
- 895 Baklanov, A., Korsholm, U., Mahura, A., Petersen, C., and Gross, A.: ENVIRO-HIRLAM: on-line coupled modelling of
896 urban meteorology and air pollution, *Adv. Sci. Res.*, 2, 41–46, doi:10.5194/asr-2-41-2008, 2008a.
- 897 Baklanov, A., Mestayer, P. G., Clappier, A., Zilitinkevich, S., Joffre, S., Mahura, A., and Nielsen, N. W.: Towards
898 improving the simulation of meteorological fields in urban areas through updated/advanced surface fluxes description,
899 *Atmos. Chem. Phys.*, 8, 523–543, doi:10.5194/acp-8-523-2008, 2008b.
- 900 Baklanov, A., Mahura, A., and Sokhi, R., eds.: *Integrated Systems of Meso-Meteorological and Chemical Transport*
901 *Models*, Springer, 242 p., doi:10.1007/978-3-642-13980-2_1, 2011a.
- 902 Baklanov, A., Schlünzen, K., Suppan, P., Baldasano, J., Brunner, D., Aksoyoglu, S., Carmichael, G., Douros, J.,
903 Flemming, J., Forkel, R., Galmarini, S., Gauss, M., Grell, G., Hirtl, M., Joffre, S., Jorba, O., Kaas, E., Kaasik, M.,
904 Kallos, G., Kong, X., Korsholm, U., Kurganskiy, A., Kushta, J., Lohmann, U., Mahura, A., Manders-Groot, A., Maurizi,
905 A., Moussiopoulos, N., Rao, S. T., Savage, N., Seigneur, C., Sokhi, R. S., Solazzo, E., Solomos, S., Sørensen, B.,
906 Tsegas, G., Vignati, E., Vogel, B., and Zhang, Y.: Online coupled regional meteorology chemistry models in Europe:
907 current status and prospects, *Atmos. Chem. Phys.*, 14, 317–398, doi:10.5194/acp-14-317-2014, 2014.
- 908 Baklanov, A., Bouchet, V., Vogel, B., Maréchal, V., Benedetti, A., and Schlünzen, K. H.: Seamless Meteorology-
909 Composition Models (SMCM): Challenges, gaps, needs and future directions. Chapter 12 in the *WWOSC Book:*
910 *Seamless Prediction of the Earth System: from Minutes to Months*, G Brunet, S Jones, PM Ruti Eds., WMO-No. 1156,
911 Geneva, 213-233, 2015.

912 Baklanov, A. A., Korsholm, U. S., Mahura, A. G., Nuterman, R. B., Sass, B. H., and Zakey, A. S.: Physical and chemical
913 weather forecasting as a joint problem: two-way interacting integrated modelling, in: American Meteorological
914 Society 91st Annual Meeting, Paper 7.1, American Meteorological Society, Seattle, WA, USA, 2011b.

915 Baklanov, A., D. Brunner, G. Carmichael, J. Flemming, S. Freitas, M. Gauss, Ø. Hov, R. Mathur, K. H. Schlünzen, C.
916 Seigneur, B. Vogel: Key issues for seamless integrated chemistry-meteorology modelling, Bulletin of the American
917 Meteorological Society. Submitted - 31 January 2016, Revised - 30 October 2016 (in press), 2017.

918 Bengtsson, L., U. Andrae, T. Aspeli, Y. Batrak, J. Calvo, W. de Rooy, E. Gleeson, B. Hansen-Sass, M. Homleid, M.
919 Hortal, K. Ivarsson, G. Lenderink, S. Niemelä, K. P. Nielsen, J. Onvlee, L. Rontu, P. Samuelsson, D. Santos Muñoz, A.
920 Subias, S. Tijm, V. Toll, X. Yang, and M. Ødegaard Kjøltzow: The HARMONIE-AROME model configuration in the
921 ALADIN-HIRLAM NWP system, *Mon. Wea. Rev.*, 145, 1919-1935, doi:10.1175/MWR-D-16-0417.1, 2017.

922 Berger A., M. Leriche, L. Deguillaume, C. Mari, P. Tulet, D. Gazen and J. Escobar: Modeling Formation of SOA from
923 Cloud Chemistry with the Meso-NH Model: Sensitivity Studies of Cloud Events Formed at the Puy de Dôme Station.
924 In: Steyn D., Chaumerliac N. (eds) Air Pollution Modeling and its Application XXIV, Springer Proceedings in
925 Complexity, Springer, Cham., 2016.

926 Bott, A.: A Positive Definite Advection Scheme Obtained by Nonlinear Renormalization of the Advective Fluxes, *Mon.
927 Weather Rew.*, 117, 1006–1016, doi:10.1175/1520-0493(1989)117<1006:APDASO>2.0.CO;2, 1989.

928 Briegleb, B. P.: Longwave band model for thermal radiation in climate studies, *J. Geophys. Res.-Atmos.*, 97, 11475–11485,
929 doi:10.1029/92JD00806, 1992.

930 Chang, J., Chang, J. S., Brost, R. A., Isaksen, I. S. A., Madronich, S., Middleton, P., Stockwell, W. R., and Walcek, C.: A
931 three-dimensional Eulerian and deposition model, Physical concepts and formulation, *J. Geophys. Res.*, 92, 14681–
932 14700, 1987.

933 Chenevez, J., Baklanov, A., and Sørensen, J. H.: Pollutant transport schemes integrated in a numerical weather
934 prediction model: model description and verification results, *Meteorol. appl.*, 11, 265–275,
935 doi:10.1017/S1350482704001343, 2004.

936 Cohard, J.-M., Pinty, J.-P., and Bedos, C.: Extending Twomey’s Analytical Estimate of Nucleated Cloud Droplet
937 Concentrations from CCN Spectra, *J. Atmos. Sci.*, 55, 3348–3357, doi:10.1175/1520-
938 0469(1998)055<3348:ETSSEO>2.0.CO;2, 1998.

939 Cohard, J.-M., Pinty, J.-P., and Suhre, K.: On the parameterization of activation spectra from cloud condensation
940 nuclei microphysical properties, *J. Geophys. Res.-Atmos.*, 105, 11753–11766, doi:10.1029/1999JD901195, 2000.

941 CORINE: Land Cover Database 2000, European Environmental Agency, [http://www.eea.europa.eu/data-and-
942 maps/data/corine-land-cover-2000-clc2000-seamless-vector-database](http://www.eea.europa.eu/data-and-maps/data/corine-land-cover-2000-clc2000-seamless-vector-database), last access: 14 June 2016.

943 Cuxart, J., Bougeault, P., and Redelsperger, J.-L.: A turbulence scheme allowing for mesoscale and large-eddy simulations, *Q.
944 J. Roy. Meteor. Soc.*, 126, 1–30, doi:10.1002/qj.49712656202, 2000.

945 de Grandpré, J., Beagley, S. R., Fomichev, V. I., Griffioen, E., McConnell, J. C., Medvedev, A. S., and Shepherd, T. G.:
946 Ozone climatology using interactive chemistry: Results from the Canadian Middle Atmosphere Model, *J. Geophys.
947 Res.-Atmos.*, 105, 26475–26491, doi:10.1029/2000JD900427, 2000.

948 Dupont, S. and Mestayer, P. G.: Parameterization of the Urban Energy Budget with the Submesoscale Soil Model, *J. Appl.
949 Meteorol. Clim.*, 45, 1744–1765, doi:10.1175/JAM2417.1, 2006.

950 Dupont, S., Mestayer, P. G., Guilloteau, E., Berthier, E., and Andrieu, H.: Parameterization of the Urban Water Budget with
951 the Submesoscale Soil Model, *J. Appl. Meteorol. Clim.*, 45, 624–648, doi:10.1175/JAM2363.1, 2006.

952 Easter, R. C.: Two Modified Versions of Bott’s Positive-Definite Numerical Advection Scheme, *Mon. Weather Rew.*,
953 121, 297–304, doi:10.1175/1520-0493(1993)121<0297:TMVOBP>2.0.CO;2, 1993.

954 Ekman, A.: Implementation of an atmospheric sulfur scheme in the HIRLAM regional weather forecast model, Report,
955 CM-96, International Meteorological Institute in Stockholm, Department of Meteorology, University of Stockholm,
956 2000.

957 Evans, M., Fiore, A., and Jacob, D.: The GEOS-CHEM chemical mechanism: Version 5-07-8, Tech. rep., University of
958 Leeds, Leeds, UK, 2003.

959 Feichter, J., Kjellström, E., Rodhe, H., Dentener, F., Lelieveld, J., and Roelofs, G.-J.: Simulation of the tropospheric sulfur
960 cycle in a global climate model, *Atmos. Environ.*, 30, 1693–1707, doi:10.1016/1352-2310(95)00394-0, 1996.

961 Feng, Y., Penner, J. E., Sillman, S., and Liu, X.: Effects of cloud overlap in photochemical models, *J. Geophys. Res.-
962 Atmos.*, 109, D04310, doi:10.1029/2003JD004040, 2004.

963 Ganzeveld, L. and Lelieveld, J.: Dry deposition parameterization in a chemistry general circulation model and its influence on
964 the distribution of reactive trace gases, *J. Geophys. Res.-Atmos.*, 100, 20999–21012, doi:10.1029/95JD02266, 1995.

965 Ganzeveld, L., Lelieveld, J., and Roelofs, G.-J.: A dry deposition parameterization for sulfur oxides in a chemistry and
966 general circulation model, *J. Geophys. Res.-Atmos.*, 103, 5679–5694, doi:10.1029/97JD03077, 1998.

967 Geoffroy, O., Brenguier, J.-L., and Burnet, F.: Parametric representation of the cloud droplet spectra for LES warm bulk
968 microphysical schemes, *Atmos. Chem. Phys.*, 10, 4835–4848, doi:10.5194/acp-10-4835-2010, 2010.

969 Gery, M. W., Whitten, G. Z., Killus, J. P., and Dodge, M. C.: A photochemical kinetics mechanism for urban and regional
970 scale computer modeling, *J. Geophys. Res.-Atmos.*, 94, 12925–12956, doi:10.1029/JD094iD10p12925, 1989.

971 Giglio, L.: Characterization of the tropical diurnal fire cycle using VIRS and MODIS observations, *Remote Sens. Environ.*,
972 108, 407–421, doi:http://dx.doi.org/10.1016/j.rse.2006.11.018, 2007.

973 González-Aparicio, I., Nuterman, R., Korsholm, U., Mahura, A., Acero, J., Hidalgo, J., and Baklanov, A.: Land-Use
974 Database Processing Approach for Meso-Scale Urban NWP Model Initialization, Tech. Rep. 10-02, Danish
975 Meteorological Institute, Copenhagen, 2010.

976 González-Aparicio, I., Hidalgo, J., Baklanov, A., Korsholm, U., Nuterman, R., Mahura, A., and Santa-Coloma, O.: Urban

977 boundary layer analysis in the complex coastal terrain of Bilbao using Enviro-HIRLAM, *Theor. Appl. Climatol.*, 113,
978 511–527, doi:10.1007/s00704-012-0808-6, 2013.

979 González-Aparicio, I., Baklanov, A., Hidalgo, J., Korsholm, U., Nuterman, R., and Mahura, A.: Impact of city
980 expansion and increased heat fluxes scenarios on the urban boundary layer of Bilbao using Enviro-HIRLAM, *Urban*
981 *Climate Journal*, 10, Part 5, 831–845, doi:10.1016/j.uclim.2014.07.010, 2014.

982 Grell, G. and Baklanov, A.: Integrated modeling for forecasting weather and air quality: A call for fully coupled approaches,
983 *Atmos. Environ.*, 45, 6845–6851, doi:10.1016/j.atmosenv.2011.01.017, 2011.

984 Grell, G. A., Peckham, S. E., Schmitz, R., McKeen, S. A., Frost, G., Skamarock, W. C., and Eder, B.: Fully coupled
985 “online” chemistry within the WRF model, *Atmos. Environ.*, 39, 6957 – 6975, doi:10.1016/j.atmosenv.2005.04.027,
986 2005.

987 Gross, A. and Baklanov, A.: Modelling the influence of dimethyl sulphide on aerosol production in the marine boundary
988 layer, *Int. J. of Environment and Pollution*, 22, 51–71, doi:10.1504/IJEP.2004.005492, 2004.

989 Guerreiro, C., de Leeuw, F., Foltescu, V., and Horálek, J.: Air quality in Europe - 2014 report, Tech. Rep. 5, European
990 Environment Agency, Copenhagen, doi:10.2800/22775, 2014.

991 Hairer, E. and Wanner, G.: Solving Ordinary Differential Equations II. Stiff and Differential-Algebraic Problems,
992 Springer-Verlag, Berlin, 2nd edn., 1996.

993 Holton, J. R.: An Introduction to Dynamic Meteorology, Elsevier academic press, Seattle, WA, USA, 4th. edn., 2004.

994 Horowitz, L. W., Walters, S., Mauzerall, D. L., Emmons, L. K., Rasch, P. J., Granier, C., Tie, X., Lamarque, J.-F., Schultz,
995 M. G., Tyndall, G. S., Orlando, J. J., and Brasseur, G. P.: A global simulation of tropospheric ozone and related tracers:
996 Description and evaluation of MOZART, version 2, *J. Geophys. Res.-Atmos.*, 108, 4784, doi:10.1029/2002JD002853,
997 2003.

998 IFS-CY40r1: <http://www.ecmwf.int/search/site/cy40r1?retain-filters=1>, last access : 13 June 2016.

999 Jacobson, M. Z.: Developing, coupling, and applying a gas, aerosol, transport, and radiation model to study urban and
1000 regional air pollution, PhD. Dissertation, Dept. of Atmospheric Sciences, UCLA, 436 pp., 1994.

1001 Jacobson, M. Z.: Studying the effects of calcium and magnesium on size-distributed nitrate and ammonium with
1002 EQUISOLV II, *Atmos. Environ.*, 33, 3635–3649, doi:10.1016/S1352-2310(99)00105-3, 1999.

1003 Jacobson, M. Z.: Control of fossil-fuel particulate black carbon plus organic matter, possibly the most effective method of
1004 slowing global warming, *J. Geophys. Res.*, 107, 4410, doi:10.1029/2001JD001376, 2002.

1005 Jantunen, J., Saarinen, K., and Rantio-Lehtimäki, A.: Allergy symptoms in relation to alder and birch pollen
1006 concentrations in Finland, *Aerobiologia*, 28, 169–176, doi:10.1007/s10453-011-9221-3, 2012.

1007 Jöckel, P., von Kuhlmann, R., Lawrence, M. G., Steil, B., Brenninkmeijer, C. A. M., Crutzen, P. J., Rasch, P. J., and Eaton,
1008 B.: On a fundamental problem in implementing flux-form advection schemes for tracer transport in 3-dimensional
1009 general circulation and chemistry transport models, *Q. J. Roy. Meteor. Soc.*, 127, 1035–1052,
1010 [doi:10.1002/qj.4971275318](https://doi.org/10.1002/qj.4971275318), 2001.

1011 Kaas, E.: A simple and efficient locally mass conserving semi-Lagrangian transport scheme, *Tellus A*, 60, 305–320, 2008.

1012 Klein, T., Kukkonen, J., Dahl, Å., Bossioli, E., Baklanov, A., Vik, A. F., Agnew, P., Karatzas, K. D., and Sofiev, M.:
1013 Interactions of physical, chemical, and biological weather calling for an integrated approach to assessment, forecasting,
1014 and communication of air quality, *Ambio*, 41, 851–864, [doi:10.1007/s13280-012-0288-z](https://doi.org/10.1007/s13280-012-0288-z), 2012.

1015 Köpke, P., Hess, M., Schult, I., and Shettle, E. P.: Global Aerosol Data Set (GADS), Tech. Rep. 243, Max-Planck-Institut
1016 für Meteorologie, Hamburg, Germany, 1997.

1017 Korsholm, U. S.: Integrated modeling of aerosol indirect effects, Ph.D. thesis, University of Copenhagen, Niels Bohr
1018 Institute and Danish Meteorological Institute, Copenhagen, Denmark, 2009.

1019 Korsholm, U. S., Baklanov, A., Gross, A., Mahura, A., Sass, B. H., and Kaas, E.: Online coupled chemical weather
1020 forecasting based on HIRLAM – overview and prospective of Enviro-HIRLAM, *HIRLAM Newsletter*, 54, 151–168,
1021 2008.

1022 Korsholm, U. S., Baklanov, A., Gross, A., and Sørensen, J. H.: On the importance of the meteorological coupling
1023 interval in dispersion modeling during ETEX-1, *Atmos. Environ.*, 43, 4805– 4810, doi:10.1016/j.atmosenv.2008.11.017,
1024 2009.

1025 Korsholm, U. S., Mahura, A., Baklanov, A., and Grell, G.: Interactions between Air Quality and Meteorology/Climate:
1026 Aerosol Feedbacks, in: FP7 MEGAPOLI Sci. Report, edited by Baklanov, A. and Mahura, A., 10-10, 31–46, 2010.

1027 Kuenen, J., Denier van der Gon, H., Visschedijk, A., van der Brugh, H., Finardi, S., Radice, P., d’Allura, A., Beevers,
1028 S., Theloke, J., Uzbasich, M., Honoré, C., and Perrussel, O.: MEGAPOLI European Gridded Emission Inventory
1029 (Final Version), MEGAPOLI Project Scientific Report, Tech. Rep. 10–17, TNO Built Environment and Geosciences,
1030 2010.

1031 Kuenen, J. J. P., Visschedijk, A. J. H., Jozwicka, M., and Denier van der Gon, H. A. C.: TNO-MACC_II emission
1032 inventory; a multi-year (2003–2009) consistent high-resolution European emission inventory for air quality modelling,
1033 *Atmos. Chem. Phys.*, 14, 10963–10976, doi:10.5194/acp-14-10963-2014, 2014.

1034 Kurganskiy, A., Mahura, A., Nuterman, R., Saarto, A., Rasmussen, A., Baklanov, A., Smyshlyayev, S., and Kaas, E.: Enviro-
1035 HIRLAM birch pollen modeling for Northern Europe, in: Report series in Aerosol Science, edited by Kulmala, M.,
1036 Zilitinkevich, S., Lappalainen, H., Kyrö, E.-M., and Kontkanen, J., vol.163, 229–234, 2015.

1037 Kurganskiy, A., Nuterman, R., Mahura, A., Kaas, E., Baklanov, A., and Sass, B.: Modelling of black and organic carbon
1038 variability in the Northern Hemisphere, in: Geophysical Research Abstracts, vol. 18, EGU2016-1404-1, 2016.

1039 Lawrence, M. G., Hov, Ø., Beekmann, M., Brandt, J., Elbern, H., Eskes, H., Feichter, H., and Takigawa, M.: The chemical
1040 weather, *Environ. Chem.*, 2, 6–8, doi:10.1071/EN05014, 2005.

1041 Linneberg, A.: The increase in allergy and extended challenges, *Allergy*, 66, 1–3, doi:10.1111/j.1398-9995.2011.02619.x,

2011.

1042 Madronich, S. and Flocke, S.: The Role of Solar Radiation in Atmospheric Chemistry, in: Environmental Photochemistry,
1043 edited by Boule, P., pp. 1–26, Springer Berlin Heidelberg, Berlin, Heidelberg, 1999.

1044 Mahura, A., Leroyer, S., Mestayer, P., Calmet, I., Dupont, S., Long, N., Baklanov, A., Petersen, C., Sattler, K., and
1045 Nielsen, N. W.: Large eddy simulation of urban features for Copenhagen metropolitan area, *Atmos. Chem. Phys.*
1046 *Discuss.*, 5, 11183–11213, doi:10.5194/acpd- 5-11183-2005, 2005a.

1047 Mahura, A., Sattler, K., Petersen, C., Amstrup, B., and Baklanov, A.: DMI-HIRLAM Modelling with High Resolution Setup
1048 and Simulations for Areas of Denmark, DMI technical report, Tech. Rep. 05-12, Copenhagen, 2005b.

1049 Mahura, A., Baklanov, A., Petersen, C., Sattler, K., Amstrup, B., and Nielsen, N. W.: ISBA Scheme Performance in High
1050 Resolution Modelling for Low Winds Conditions, *HIRLAM Newsletter*, 49, 22–35, 2006a.

1051 Mahura, A., Baklanov, A., Rasmussen, A., Korsholm, U., and Petersen, C.: Birch pollen forecasting for Denmark, in:
1052 Abstracts of 6th Annual Meeting of European Meteorological Society (EMS), vol. 3, EMS2006-A-00495, 3-7 Sep.,
1053 Ljubljana, Slovenia, 2006b.

1054 Mahura, A., Baklanov, A., Hoe, S., Sorensen, J. H., Petersen, C., and Sattler, K.: Evaluation of land surface scheme
1055 modifications on atmospheric transport and deposition patterns in Copenhagen metropolitan area, in: Air Pollution
1056 Modeling and Its Application XVIII, edited by Borrego, C. and Renner, E., vol. 6 of Developments in
1057 Environmental Science, Elsevier, 64–72, doi:10.1016/S1474-8177(07)06017-2, 2007a.

1058 Mahura, A., Korsholm, U., Baklanov, A., and Rasmussen, A.: Elevated birch pollen episodes in Denmark: contributions from
1059 remote sources, *Aerobiologia*, 23, 171–179, doi:10.1007/s10453-007-9061-3, 2007b.

1060 Mahura, A., Leroyer, S., Baklanov, A., Mestayer, P., Korsholm, U., and Calmet, I.: Temporal and Spatial Variability of
1061 Fluxes in Urbanized Areas, in: Urban Climate and Bioclimate, pp. 219–232, 2008a.

1062 Mahura, A., Petersen, C., Baklanov, A., and Amstrup, B.: Evaluation of Building Effect Parameterization Module for
1063 Urbanized Numerical Weather Prediction Modelling, in: Urban Climate and Bioclimate, pp. 371–380, 2008b.

1064 Mahura, A., Petersen, C., Baklanov, A., Amstrup, B., Korsholm, U. S., and Sattler, K.: Verification of Long-term DMI-
1065 HIRLAM NWP Model Runs Using Urbanisation and Building Effect Parameterization Modules, *HIRLAM Newsletter*,
1066 53, 50–60, 2008c.

1067 Mahura, A., Baklanov, A., and Korsholm, U.: Parameterization of the birch pollen diurnal cycle, *Aerobiologia*, 25,
1068 203–208, doi:10.1007/s10453-009-9125-7, 2009.

1069 Mahura, A., Korsholm, U., Baklanov, A., Petersen, C., and Rasmussen, A.: Birch Pollen: Modelling, Spatial and
1070 Temporal Variability, Elevated Episodes, Potential Source Regions, Emissions Parametrizations, and Future Research, in:
1071 Abstracts of International Conference on Environmental Observations, Modeling and Information Systems
1072 (ENVIROMIS-2010), pp. 87–88, 5-11 Jul., Tomsk, Russia, 2010a.

1073 Mahura, A., Nuterman, R., Gonzalez-Aparicio, I., Petersen, C., and Baklanov, A.: Environmental modelling in Metropolitan
1074 Areas, DMI Sci. Report, Tech. Rep. 10-06, 2010b.

1075 Mahura, A., Nuterman, R., Gonzalez-Aparicio, I., Amstrup, B., Yang, X., and Baklanov, A.: Meteorological and
1076 Chemical Urban Scale Modelling for Shanghai Metropolitan Area, in: Geophysical Research Abstracts, vol. 18,
1077 EGU2016-1394, 2016.

1078 Mahura, A., Amstrup, B., Nuterman, R., Yang, X., Baklanov, A.: Multi-Scale Enviro-HIRLAM Forecasting of Weather
1079 and Atmospheric Composition over China and its Megacities, in: Geophysical Research Abstracts, Vol. 19, EGU2017-
1080 9564, 2017.

1081 Marchuk, G. I.: Mathematical models in environmental problems, in: Studies in mathematics and its applications, 16,
1082 Elsevier Sci. Pub. Co. ISBN 044487965X, 217 pp., 1986.

1083 Martilli, A., Clappier, A., and Rotach, M. W.: An Urban Surface Exchange Parameterisation for Mesoscale Models,
1084 *Bound.-Layer Meteor.*, 104, 261–304, doi:10.1023/A:1016099921195, 2002.

1085 Mayer, B. and Kylling, A.: Technical note: The libRadtran software package for radiative transfer calculations - description
1086 and examples of use, *Atmos. Chem. Phys.*, 5, 1855–1877, doi:10.5194/acp-5-1855-2005, 2005.

1087 Nightingale, P. D., Malin, G., Law, C. S., Watson, A. J., Liss, P. S., Liddicoat, M. I., Boutin, J., and Upstill-Goddard, R.
1088 C.: In situ evaluation of air-sea gas exchange parameterizations using novel conservative and volatile tracers, *Global*
1089 *Biogeochem. Cy.*, 14, 373–387, doi:10.1029/1999GB900091, 2000.

1090 Noilhan, J. and Planton, S.: A Simple Parameterization of Land Surface Processes for Meteorological Models, *Mon.*
1091 *Weather Rew.*, 117, 536–549, doi:10.1175/1520-0493(1989)117<0536:ASPOLS>2.0.CO;2, 1989.

1092 Nuterman, R., Korsholm, U., Zakey, A., Nielsen, K. P., Sørensen, B., Mahura, A., Rasmussen, A., Mažeikis, A.,
1093 Gonzalez-Aparicio, I., Morozova, E., Sass, B. H., Kaas, E., and Baklanov, A.: New developments in Enviro-HIRLAM
1094 online integrated modeling system, in: Geophysical Research Abstracts, vol. 15, EGU2013-12520-1, 2013.

1095 Nuterman, R., Mahura, A., Baklanov, A., Kurganskiy, A., Amstrup, B., and Kass, E.: Enviro-HIRLAM Applicability
1096 for Black Carbon Studies in Arctic, in: Geophysical Research Abstracts, vol. 17, EGU2015-1571, 2015.

1097 Päävinen, R., Lehtikainen, M., Schuck, A., Häme, T., Väätäinen, S., Kennedy, P., and Folving, S.: Combining Earth
1098 Observation Data and Forest Statistics, Tech. Rep. 14, EFI, Joensuu and Joint Research Centre / European Commission,
1099 2001.

1100 Penenko, V. V. and Aloyan, A. E.: Models and methods for environment protection problems, Nauka, Novosibirsk, 1985
1101 (in Russian).

1102 Rasch, P. J. and Kristjansson, J. E.: A Comparison of the CCM3 Model Climate Using Diagnosed and Predicted
1103 Condensate Parameterizations, *J. Climate*, 11, 1587–1614, doi:10.1175/1520-0442(1998)011<1587:ACOTCM>2.0.CO;2,
1104 1998.

1105 Rasmussen, A.: The effects of climate change on the birch pollen season in Denmark, *Aerobiologia*, 18, 253–265,
1106

doi:10.1023/A:1021321615254,2002.

1108 Rasmussen, A., Mahura, A., Baklanov, A., and Sommer, J.: The Danish Operation Pollen Forecasting System, in:
1109 Abstracts of 8th International Congress on Aerobiology "Towards a comprehensive vision", p. 179, Neuchâtel,
1110 Switzerland, 21-25 Aug., 2006.

1111 Robert, A.: A stable numerical integration scheme for the primitive meteorological equations, *Atmos.-Ocean*, 19, 35–46,
1112 doi:10.1080/07055900.1981.9649098, 1981.

1113 Sass, B. H.: A research version of the STRACO cloud scheme, Tech. Rep. 02-10, Danish Meteorological Institute,
1114 Copenhagen, 2002.

1115 Sander, S. P., Friedl, R. R., Golden, D. M., Kurylo, M. J., Huie, R. E., Orkin, V. L., Moortgat, G. K., Ravishankara, A. R.,
1116 Kolb, C. E., Molina, M. J., and Finlayson-Pitts, B. J.: Chemical kinetics and photochemical data for use in stratospheric
1117 modeling. Evaluation No. 14, JPL 02-25, 2003.

1118 Sandu, A. and Sander, R.: Technical note: Simulating chemical systems in Fortran90 and Matlab with the Kinetic
1119 PreProcessor KPP-2.1, *Atmos. Chem. Phys.*, 6, 187–195, doi:10.5194/acp-6-187-2006, 2006.

1120 Sandu, A., Verwer, J. G., Blom, J. G., Spee, E. J., Carmichael, G. R., and Potra, F. A.: Benchmarking stiff ODE solvers for
1121 atmospheric chemistry problems II: Rosenbrock solvers, *Atmos. Environ.*, 31, 3459–3472, 1997.

1122 Savijärvi, H.: Fast Radiation Parameterization Schemes for Mesoscale and Short-Range Forecast Models, *J. Appl.*
1123 *Meteorol.*, 29, 437–447, doi:10.1175/1520-0450(1990)029<0437:FRPSFM>2.0.CO;2, 1990.

1124 Schlünzen, K. H. and Pahl, S.: Modification of dry deposition in a developing sea-breeze circulation – a numerical case
1125 study, *Atmos. Environ.*, 26, 51–61, 1992.

1126 Seifert, A. and Beheng, D. K.: A two-moment cloud microphysics parameterization for mixed-phase clouds. Part 1:
1127 Model description, *Meteorol. Atmos. Phys.*, 92, 45–66, doi:10.1007/s00703-005-0112-4, 2006.

1128 Seinfeld, J. and Pandis, S.: *Atmospheric Chemistry and Physics: From Air Pollution to Climate Change*, A Wiley-
1129 Interscience publication, Wiley, 1st edn., 1998.

1130 Seinfeld, J. and Pandis, S.: *Atmospheric Chemistry and Physics: From Air Pollution to Climate Change*, A Wiley-
1131 Interscience publication, Wiley, 2nd edn., 2006.

1132 Shalaby, A.: Coupling of Regional Climate Chem Aerosol Model, Ph.D. thesis, Faculty of Science, Cairo University,
1133 Egypt, 2012.

1134 Shalaby, A., Zakey, A. S., Tawfik, A. B., Solmon, F., Giorgi, F., Stordal, F., Sillman, S., Zaveri, R. A., and Steiner, A. L.:
1135 Implementation and evaluation of online gas-phase chemistry within a regional climate model (RegCM-CHEM4),
1136 *Geosci. Model Dev.*, 5, 741-760, doi:10.5194/gmd-5-741-2012, 2012.

1137 Siljamo, P., Sofiev, M., Filatova, E., Grewling, L., Jäger, S., Khoreva, E., Linkosalo, T., Ortega Jimenez, S., Ranta, H.,
1138 Rantio-Lehtimäki, A., Svetlov, A., Veriankaite, L., Yakovleva, E., and Kukkonen, J.: A numerical model of birch
1139 pollen emission and dispersion in the atmosphere. Model evaluation and sensitivity analysis, *Int. J. Biometeorol.*, 57,
1140 125–136, doi:10.1007/s00484-012-0539-5, 2013.

1141 Sillman, S.: A numerical solution for the equations of tropospheric chemistry based on an analysis of sources and sinks of
1142 odd hydrogen, *J. Geophys. Res.-Atmos.*, 96, 20735–20744, doi:10.1029/91JD01967, 1991.

1143 Skjøth, C. A., Geels, C., Hvidberg, M., Hertel, O., Brandt, J., Frohn, L. M., Hansen, K. M., Hedegaard, G. B.,
1144 Christensen, J. H., and Moseholm, L.: An inventory of tree species in Europe - An essential data input for air pollution
1145 modelling, *Ecol. Model.*, 217, 292–304, doi:10.1016/j.ecolmodel.2008.06.023, 2008.

1146 Sofiev, M., Siljamo, P., Ranta, H., and Rantio-Lehtimäki, A.: Towards numerical forecasting of long-range air transport
1147 of birch pollen: theoretical considerations and a feasibility study, *Int. J. Biometeorol.*, 50, 392–402, doi:10.1007/s00484-
1148 006-0027-x, 2006.

1149 Sofiev, M., Siljamo, P., and Khvorostyanov, D.: Validation report of PBAP routine in SILAM and R-ENS models, Tech. Rep.
1150 D_R-ENS_1.7.4, 2011.

1151 Sofiev, M., Ermakova, T., and Vankevich, R.: Evaluation of the smoke-injection height from wild-land fires using
1152 remote-sensing data, *Atmos. Chem. Phys.*, 12, 1995–2006, doi:10.5194/acp-12-1995-2012, 2012.

1153 Sofiev, M., Siljamo, P., Ranta, H., Linkosalo, T., Jaeger, S., Rasmussen, A., Rantio-Lehtimäki, A., Severova, E., and
1154 Kukkonen, J.: A numerical model of birch pollen emission and dispersion in the atmosphere. Description of the emission
1155 module, *Int. J. Biometeorol.*, 57, 45–58, doi:10.1007/s00484-012-0532-z, 2013.

1156 Sokhi, R., Baklanov, A., Schlunzen, H., eds.: *Air Pollution and Meteorological Modelling for Atmospheric Research and*
1157 *Policy Applications*, Anthem Press, in press, 260 pp., 2017.

1158 Sørensen, B.: New mass conserving multi-tracer efficient transport schemes focusing on semi-Lagrangian and Lagrangian
1159 methods for online integration with chemistry, Ph.D. thesis, University of Copenhagen, Niels Bohr Institute and Danish
1160 Meteorological Institute, Copenhagen, Denmark, 2012.

1161 Sørensen, B., Kaas, E., and Korsholm, U. S.: A mass-conserving and multi-tracer efficient transport scheme in the online
1162 integrated Enviro-HIRLAM model, *Geosci. Model Dev.*, 6, 1029–1042, doi:10.5194/gmd-6-1029-2013, 2013.

1163 Stamnes, K., Tsay, S.-C., Wiscombe, W., and Jayaweera, K.: Numerically stable algorithm for discrete-ordinate-method
1164 radiative transfer in multiple scattering and emitting layered media, *Appl. Opt.*, 27, 2502–2509,
1165 doi:10.1364/AO.27.002502, 1988.

1166 Steil, B., Brühl, C., Manzini, E., Crutzen, P. J., Lelieveld, J., Rasch, P. J., Roeckner, E., and Krüger, K.: A new interactive
1167 chemistry-climate model: 1. Present-day climatology and interannual variability of the middle atmosphere using the
1168 model and 9 years of HALOE/UAARS data, *J. Geophys. Res.-Atmos.*, 108, 4290, doi:10.1029/2002JD002971, 2003.

1169 Stier, P., Feichter, J., Kinne, S., Kloster, S., Vignati, E., Wilson, J., Ganzeveld, L., Tegen, I., Werner, M., Balkanski, Y.,
1170 Schulz, M., Boucher, O., Minikin, A., and Petzold, A.: The aerosol-climate model ECHAM5-HAM, *Atmos. Chem.*
1171 *Phys.*, 5, 1125–1156, doi:10.5194/acp-5-1125-2005, 2005.

1172 Stockwell, W. R., Kirchner, F., Kuhn, M., and Seefeld, S.: A new mechanism for regional atmospheric chemistry
1173 modeling, *J. Geophys. Res.-Atmos.*, 102, 25847–25879, doi:10.1029/97JD00849, 1997.
1174 Thomas, G. E. and Stamnes, K.: *Radiative Transfer in the Atmosphere and Ocean*, Cambridge University Press, New York,
1175 NY, USA, 2002.
1176 Twomey, S.: The nuclei of natural cloud formation part II: The supersaturation in natural clouds and the variation of cloud
1177 droplet concentration, *Geophys. Pure Appl.*, 43, 243–249, doi:10.1007/BF01993560, 1959.
1178 Undén, P., Rontu, L., Järvinen, H., Lynch, P., Calvo, J., Cats, G., Cuxart, J., Eerola, K., Fortelius, C., Garcia-Moya, J. A.,
1179 Jones, C., Lenderlink, G., McDonald, A., Mc-Grath, R., Navascues, B., Nielsen, N. W., Øidegaard, V., Rodriguez, E.,
1180 Rummukainen, M., Rööm, R., Sattler, K., Sass, B. H., Savijärvi, H., Schreur, B. W., Sigg, R., The, H., and Tijn, A.:
1181 HIRLAM-5 Scientific Documentation, Tech. rep., The HIRLAM project, Norrköping, Sweden, 2002.
1182 Vignati, E., Wilson, J., and Stier, P.: M7: An efficient size-resolved aerosol microphysics module for large-scale aerosol
1183 transport models, *J. Geophys. Res.-Atmos.*, 109, D22202, doi:10.1029/2003JD004485, 2004.
1184 WHO: Phenology and human health: allergic disorders, Tech. rep., WHO Regional Office for Europe, Copenhagen, Denmark,
1185 2003.
1186 WMO: Coupled Chemistry-Meteorology/Climate Modelling (CCMM): status and relevance for numerical weather
1187 prediction, atmospheric pollution and climate research (Symposium materials). WMO GAW Report #226, WMO,
1188 Geneva, Switzerland, https://www.wmo.int/pages/prog/arep/gaw/documents/Final_GAW_226_10_May.pdf, 2016.
1189 WMO-COST: Joint Report of COST Action 728 and GURME - Overview of Existing Integrated (off-line and on-line) Mesoscale
1190 Meteorological and Chemical Transport Modelling Systems in Europe (WMO TD No. 1427), GAW report 177, 106 pp, May
1191 2008, http://library.wmo.int/pmb_ged/wmo-td_1427.pdf, 2008.
1192 Wild, O., Zhu, X., and Prather, M. J.: Fast-J: Accurate Simulation of In- and Below-Cloud Photolysis in Tropospheric
1193 Chemical Models, *J. Atmos. Chem.*, 37, 245–282, doi:10.1023/A:1006415919030, 2000.
1194 Wyser, K., Rontu, L., and Savijärvi, H.: Introducing the effective radius into a fast radiation scheme of a mesoscale
1195 model, *Contr. Atmos. Phys.*, 72, 205–218, 1999.
1196 Zakey, A. S., Solmon, F., and Giorgi, F.: Implementation and testing of a desert dust module in a regional climate model,
1197 *Atmos. Chem. Phys.*, 6, 4687–4704, doi:10.5194/acp-6-4687-2006, 2006.
1198 Zakey, A. S., Giorgi, F., and Bi, X.: Modeling of sea salt in a regional climate model: Fluxes and radiative forcing, *J.*
1199 *Geophys. Res.-Atmos.*, 113, D14221, doi:10.1029/2007JD009209, 2008.
1200 Zaveri, R. A. and Peters, L. K.: A new lumped structure photochemical mechanism for large-scale applications, *J.*
1201 *Geophys. Res.-Atmos.*, 104, 30387–30415, doi:10.1029/1999JD900876, 1999.
1202 Zhang, Y.: Online-coupled meteorology and chemistry models: history, current status, and outlook, *Atmos. Chem. Phys.*,
1203 8, 2895–2932, doi:10.5194/acp-8-2895-2008, 2008.
1204 Zilitinkevich, S. and Baklanov, A.: Calculation Of The Height Of The Stable Boundary Layer In Practical Applications,
1205 *Bound.-Layer Meteor.*, 105, 389–409, doi:10.1023/A:1020376832738, 2002.
1206 Zilitinkevich, S., Baklanov, A., Rost, J., Smedman, A.-S., Lykosov, V., and Calanca, P.: Diagnostic and prognostic
1207 equations for the depth of the stably stratified Ekman boundary layer, *Q. J. Roy. Meteor. Soc.*, 128, 25–46,
1208 doi:10.1256/00359000260498770, 2002.

1209 1210 1211 1212 **Annex 1: Enviro-HIRLAM model development history:**

1213
1214 1999: Started at DMI as an unfunded initiative (A. Baklanov et al.)
1215 2000: Used previous experience of the Novosibirsk scientific school (A. Baklanov) and SMHI (A. Ekman PhD)
1216 2001: Online passive pollutant transport and deposition in HIRLAM-Tracer (J. Chenevez, A. Baklanov, J.H. Sørensen)
1217 2003: Aerosol dynamics model developed and tested first as OD module in offline CAC (A. Baklanov, A. Gross)
1218 2004: Test of different formulations for advection of tracers incl. cloud water (K. Lindberg)
1219 2005: Urbanisation of the model (funded by FP5 FUMAPEX) (A. Baklanov, A. Mahura, C. Peterson)
1220 2005: COGCI grant for PhD study of aerosol feedbacks in Enviro-HIRLAM (U. Korsholm, supervised by A. Baklanov, E.
1221 Kaas)
1222 2006: Test of CISL scheme in Enviro-HIRLAM (P. Lauritzen, K. Lindberg)
1223 2007: First version of Enviro-HIRLAM for pollen studies (A. Mahura, U. Korsholm, A. Rasmussen, A. Baklanov)
1224 2008: New economical chemical solver NWP-Chem (A. Gross)
1225 2008: First version of Enviro-HIRLAM with indirect aerosol feedbacks (U. Korsholm PhD)
1226 2008: Testing new advection schemes in Enviro-HIRLAM (UC: E. Kaas, A. Christensen, B. Sørensen, J.R. Nielsen)
1227 2008: Decision to build HIRLAM Chemical Branch (HCB) with Enviro-HIRLAM as baseline system, Enviro-HIRLAM
1228 becomes an international project
1229 2008: 1st International Young Scientist Summer School (YSSS) on “Integrated Modelling of Meteorological and Chemical
1230 Transport Processes” (based on Enviro-HIRLAM) in St. Petersburg, Russia: <http://netfam.fmi.fi/YSSS08/>
1231 2009: Integrated version of Enviro-HIRLAM based on reference version 7.2 and HCB start
1232 2011: New chemistry (A. Zakey), direct and semi-direct aerosols effect (K.P. Nielsen) schemes
1233 2011: 2nd International YSSS based on Enviro-HIRLAM/HARMONIE) in Odessa, Ukraine: <http://www.ysss.osenu.org.ua/>
1234 2012: New effective aerosol scheme for multi-compound aerosols (R. Nuterman)
1235 2012: New mass conserving and monotonic semi-Lagrangian transport (B. Sørensen et al. 2013)
1236 2013: New STRACO scheme with aerosol-clouds interaction (U. Korsholm and B. Sass)

1237 2013: Model evaluation study within the AQMEII, phase 2 exercise (R. Nuterman)
 1238 2014: Moving to the HARMONIE platform and building a joint strategy with ALADIN community
 1239 2014: 3rd International YSSS (based on 5 online coupled models including Enviro-HIRLAM/HARMONIE) in Aveiro,
 1240 Portugal: <http://aveiroschool2014.web.ua.pt/>
 1241 2014-2016: Enviro-HIRLAM birch pollen forecasting system (A. Kurganskiy et al.)
 1242 2015: New radiation scheme with aerosol direct and semi-direct effects for SW and LW radiation (K.P. Nielsen et al.)
 1243 2016: Application of Enviro-HIRLAM for China (Marco-Polo project, A. Mahura et al.)
 1244

1245 **Annex 2: Abbreviations and acronyms used in this article:**
 1246

1247	ACT	Atmospheric chemical transport
1248	AHF	Anthropogenic heat flux
1249	ALADIN	Aire Limitée (pour l') Adaptation dynamique (par un) Développement InterNational (model and consortium)
1250	AOD	Aerosol Optical Depth
1251	AQ	Air Quality
1252	AQMEII	Air Quality Model Evaluation International Initiative
1253	AROME	Application of Research to Operations at Mesoscale-model (Météo-France) ARW. The Advanced Research WRF solver (dynamical core)
1254	BC	Black Carbon
1255	BEP	Building Effect Parameterization
1256	CAC	Chemistry-Aerosol-Cloud model (tropospheric box model)
1257	CarboNord	Nordic project "Impact of Black Carbon on Air Quality and Climate in Northern Europe and Arctic"
1258	CBM-IV	The modified implementation of the Carbon Bond Mechanism version IV
1259	CBM-Z	CBM-Z extends the CBM-IV to include reactive long-lived species and their intermediates, isoprene chemistry, optional DMS chemistry
1260	CHIMERE	A multi-scale CTM for air quality forecasting and simulation
1261	CISL	Cell-integrated semi-Lagrangian (transport scheme)
1262	COGCI	Copenhagen Global Climate Initiative
1263	CORINE	European land-use database
1264	COST	European Cooperation in Science and Technology (http://www.cost.eu/)
1265	COSMO	Consortium for Small-Scale Modelling
1266	COSMO-ART	COSMO + Aerosols and Reactive Trace gases
1267	CPU	Central Processing Unit
1268	CRAICC-PEEX	CRyosphere-Atmosphere Interactions in a Changing Arctic Climate - Pan Eurasian EXperiment
1269	CRUCIAL	Nordic project "Critical steps in understanding land surface atmosphere interactions: from improved knowledge to socioeconomic solutions"
1270	CTM	Chemistry-Transport Model
1271	CWF	Chemical Weather Forecasting
1272	DMI	Danish Meteorological Institute
1273	DMS	Dimethyl sulphide
1274	DEHM	Danish Eulerian Hemispheric Model
1275	ECMWF	European Centre of Medium-Range Weather Forecasts
1276	EFI	European Forest Institute
1277	ECHAM5-HAM	Global aerosol-climate model: Global GCM ECHAM (version 5) + Aerosol chemistry and microphysics package HAM (MPI for Meteorology, Hamburg)
1278	ENCWF	European Network on Chemical Weather Forecasting
1279	Enviro-HIRLAM	High Resolution Limited Area Model HIRLAM with chemistry (DMI and collaborators)
1280	EnviroRISKS	EU FP6 project: 'Environmental Risks: Monitoring, Management and Remediation of Man-made Changes in Siberia'
1281	EPA	USA Environmental Protection Agency
1282	ESM	Earth System Modelling
1283	EuMetChem	The COST Action ES1004 – European framework for online integrated air quality and meteorology modelling (eumetchem.info)
1284	ETEX	European Tracer Experiment
1285	FAR	False alarm ratio
1286	FMI	Finnish Meteorological Institute
1287	FP5.7	European Union Framework Programs
1288	FUMAPEX	EU FP5 project "Integrated Systems for Forecasting Urban Meteorology, Air Pollution and Population Exposure"
1289	GADS	Global Aerosol Data Set
1290	GAW	Global Atmosphere Watch (WMO Programme)
1291	GEOS-Chem	GEOS-Chem is a global 3-D chemical transport model (CTM) for atmospheric composition driven by meteorological input from the Goddard Earth Observing System (GEOS) of the NASA Global Modeling and Assimilation Office
1292	GIS	Geographical Information System
1293	GLCC	Global Land Cover Characterization
1294	HAM	Simplified global primary aerosol mechanism model
1295	HARMONIE	Hirlam Aladin Research on Meso-scale Operational NWP in Europe (model)
1296	HCb	HIRLAM Chemical Branch
1297	HIRLAM	High Resolution Limited Area Model (http://hirlam.org/)
1298	HR	Hit rate
1299	IC/BC	Initial / Boundary Conditions
1300	IFS	Integrated Forecast System (ECMWF)
1301	ILMC	Posteriori iterative locally mass-conserving filter
1302	ISBA	Interaction Soil- Biosphere- Atmosphere land surface scheme
1303	IS4FIRES	Global biomass burning (wildfires) emission inventory developed by FMI
1304	KPP	Kinetic Pre-Processors
1305	LAI	Leaf Area Index
1306	LMCSL	Locally Mass Conserving Semi-Lagrangian scheme
1307	LUCY	Large scale Urban Consumption of energy model
1308	LW	Long-wave radiation
1309	MA	Model accuracy
1310	M7	Modal aerosol model
1311	MACC	Monitoring Atmospheric Composition and Climate (EU project)
1312	MEGAPOLI	EU FP7 project 'Megacities: Emissions, urban, regional and Global Atmospheric POLLution and climate effects, and Integrated tools for assessment and mitigation' (http://megapoli.info/)
1313	MESO-NH	Non-hydrostatic mesoscale atmospheric model (French research community)
1314	MetM	Meteorological prediction model
1315	MOZART	Model for Ozone And Related Tracers (global CTM)
1316	NetFAM	Nordic Research Network on Fine-scale Atmospheric Modelling
1317	NMVOG	Non-Methane Volatile Organic Compounds
1318	NWP	Numerical Weather Prediction
1319	OC	Organic Carbon
1320	ODE	Ordinary Differential Equation
1321	OR	Odds ratio
1322	PBL	Planetary Boundary Layer
1323	POFD	Probability of false detection
1324	OPAC	Optical Properties of Aerosols and Clouds (software library module)
1325	PEGASOS	EU FP7 project: Pan-European Gas-Aerosol-Climate interaction study (http://pegasos.iceht.forth.gr/)
1326	PM	Particulate Matter in two size bins – 2.5 µm and 10 µm (PM _{2.5} and PM ₁₀)
1327	RBM	Radical balance method
1328	RACM	Regional Atmospheric Chemistry Mechanism
1329	SL	Semi-Lagrangian scheme
1330	SMHI	Swedish Meteorological and Hydrological Institute

